The Removal of Lead Ions from Water Using Thiophene-Containing Metal-Organic Frameworks

by

Alissa Renee Geisse

Submitted in Partial Fulfillment of the Requirements

for the Degree of

Master of Science

in the

Chemistry

Program

YOUNGSTOWN STATE UNIVERSITY

August 2019

The Removal of Lead Ions from Water Using Thiophene-Functionalized Metal-Organic Frameworks

Alissa Renee Geisse

I hereby release this thesis to the public. I understand that this thesis will be made available from the OhioLINK ETD Center and the Maag Library Circulation Desk for public access. I also authorize the University or other individuals to make copies of this thesis as needed for scholarly research.

Signature:

_____

_____ *Alissa R. Geisse*, Student Date

Approvals:

_____

_____ *Dr. Douglas T Genna*, Thesis Advisor Date

_____

_____ *Dr. Brian D. Leskiw*, Committee Member Date

_____

_____ *Dr. Nina V. Stourman*, Committee Member Date

_____

_____ Dr. Salvatore A. Sanders, Dean of Graduate Studies Date

Acknowledgments

My experience within the chemistry department at Youngstown State University has been both invaluable and agreeable. The faculty look towards not only bettering a student's chemical understanding, but also are always compassionate and willing to impart "life advice." I have also had the pleasure of growing alongside my fellow graduate students, and although some of them moved-on to graduate school a year before me, I treasure our friendship and always look forward to our reunions. Thank you, Joe S., Joe P., Sarah, Matt and Larry. I wish you all the best of luck in your future endeavors.

I would also like to personally thank my two additional committee members Dr. Stourman and Dr. Leskiw. In different ways, you both serve as role models to me. Also, it remains tastefully ironic to myself that you both remain the only two professors I had as an undergraduate in whose classes I truly struggled … and yet here we are. Hopefully I can prove to you both some inkling of academic growth (just maybe not in physical chemistry). Thank you both for your outside perspectives on this project - I look up to your expertise in your individual fields.

I feel as though I could write a thesis-length document on my many thanks to my mentor, Dr. Genna, alone. His first year at YSU was when I started taking organic chemistry, and as if learning Ochem for the first time was not thought-provoking enough, this guy made recitation feel like mental Olympics (in a good way). He and Dr. Norris combined had invigorated within me a deep love for chemistry, specifically the building and designing of molecules. I am very grateful towards both that I am not currently enrolled in pharmacy school.

Second, I would like to thank Dr. Genna for seeing the potential in me as a scientist. The abilities and expertise I have gained through him are many, and I feel best prepared for the next step. He imparted on me an appreciation for staying current in scientific literature, how to present personal research in both a professional and meaningful way, how to write manuscripts and grants, and even how to mentor other students. Dr. Genna's work ethic and enthusiasm for his profession is both inspiring and commendable. He has provided me with an image to strive to be like, and someone to look up to. "It's not about how you start; it is about how you finish". Thank you for believing in me. Godspeed Bro Doug.

I would also like to quickly thank Dr. Jackson for the time he served as my TA advisor. I had learned a lot from him during our meetings, specifically on lab techniques and how to best guide students through difficult scenarios.

To my best friend Logan: coming to Youngstown State University had given me the chance to become your best friend. I will still never understand how you as a fashion major could predict organic reactions better than myself but thank you for your intuitive chemical insight. For the last 5 years we have done absolutely everything together, from quitting our jobs to travelling foreign countries, and it is time for our paths to diverge. Thank you for all the support and seeing me through both my best and worst of times.

To the whole Genna Lab, you have provided me with a true sense of family. I have loved learning from those before me, as well as watching those after me grow in their own chemical understanding. I have enjoyed our spontaneous lunch and coffee trips, paint and sips, and fellowship at lab dinners. Without you guys, I wouldn't know what to do. I wish the best for all of you.

ABSTRACT

The work herein employs thiophene-containing metal-organic frameworks (MOFs) as an aqueous lead adsorbent both in batch and flow reactions. This thesis seeks to identify an ideal MOF system for lead ion removal from water. Evidence herein supports that the thiophene moiety is capable of lead ion binding both as a solid support (within MOFs) and in solution (observed via NMR). A thiophene-containing MOF, DUT-67, was proven to bind lead both in batch and in flow reactions, and was able to be regenerated/recycled for 5 consecutive flow reactions at 21 ppm lead. Through modeling, integration of DUT-67's experimental breakthrough curve, and solution-state lead NMR, there exhibits strong evidence for a thiophene-Pb plumbacene interaction. To our knowledge, this is the first time this interaction has been reported.

Table of Contents

List of Figures

List of Tables

Chapter 1: Introduction

Water Contamination

Both local and natural water has been under the assault of anthropogenic-derived contamination for many years. Humankind has been unknowingly and/or carelessly polluting water with contaminants such as polyaromatic hydrocarbons (PAHs),[1] perflourinated organics (PFOs),[2] pharmaceuticals and their biological metabolites,[3] and heavy metals.[4] In fact, this pressing issue concerning the lack of useable water has gained attention across social and news media as the "water crisis." According to a non-profit organization known as The Water Project:[5] dirty water conditions kill one child every 15 seconds, and over 1 billion people worldwide still lack access to safe water. Half of the world's hospital beds are occupied by people suffering from a water-related disease,[6] and in developing countries, as much as 80% of illnesses are linked to poor/sanitary water conditions.[5] **Figure 1** depicts some of the most common water contaminants.

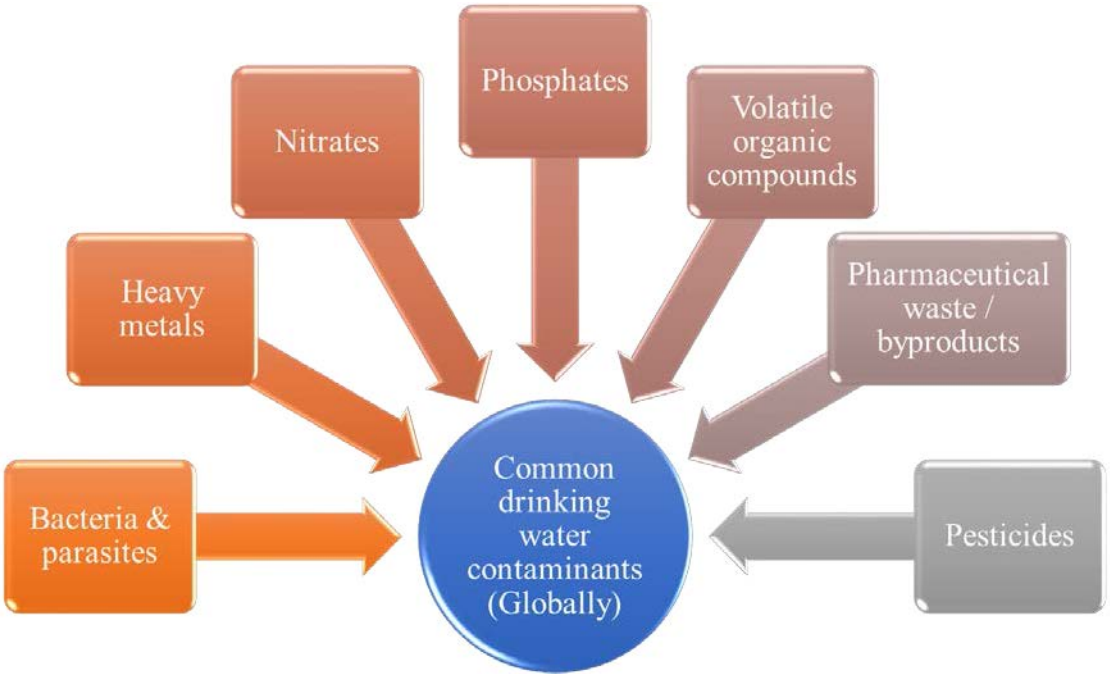

Figure 1: Common drinking water contaminants

The onset of the Industrial Revolution which began in the 18th century only intensified water pollution. This was a period of grand economic development and was marked by the invention of power-driven machinery. Factories began to proliferate, and from these factories industrial waste was released without prior treatment into natural water bodies like rivers, streams, lakes, and oceans.[7] However, it is not only the past release of persistent chemical waste into the environment which possesses an issue, but also aging infrastructure which is constantly degrading and leaching contaminants as time progresses. In the last 50 years, an exponential increase in the use of heavy metals in industrial processes and products such as metal plating facilities, mining operations, tanneries, and fertilizers has afforded a slow leaching of heavy metals into the environment.[8] Specifically, heavy metals such as mercury, arsenic, cadmium and lead have become a growing problem on the global scale.[9] Heavy metal leeching has been shown to cause detrimental effects on soil, plants, aquatic environments, and on human health.[4] Unlike most organic contaminants, heavy metals are not easily biodegradable and tend to accumulate in living organisms.[10]

Lead-Water Contamination

Lead, although ubiquitous in our environment, has not been found to play a physiological role in biological systems. For centuries, lead toxicity has been one of the most impactful and preventable causes of neurological morbidity from an environmental contaminate. The EPA had established that the federal limit for lead in drinking water is 15 ppb, and if more than 10% of consumer tap water exceeds this limit than the public must be informed of the steps they can take in order to protect their family's health.[11] Lead-water contamination has gained a lot of attention due to the Flint, Michigan water crisis in 2014,[12]

where lead had started leaching into the community's water from the pipes in which the water was transported. Not only did the Flint water crisis pose a threat on the people that reside there, but it also had a profound effect on the level of trust within the community with the water utility industry.

Naturally occurring anthropogenic behavior and metal leeching from industrially produced goods have contributed to an increase in the concentration of lead in the environment. Lead is still currently processed to make lead-acid batteries, munitions, X-ray shields, ceramics, paint, caulking, and pipe solder.[13] Industrial occupations concerning the processing and manufacturing of these goods are the primary source of chronic lead exposure. Lead leeching into the environment in its ionic state can be particularly dangerous because it accumulates throughout the entirety of food chains. When lead and other heavy metals are first released into the environment, they will accumulate in the bodies of small water organisms like phytoplanktons, as well as soil organisms such as the microbial community.[14] Both soil microbes and phytoplanktons are important keystone species which affect biocommunity structure and biodiversity by recycling plant nutrients and maintaining soil structure. A poisoning of these small organisms causes an increase in heavy metal concentration in soil and water where the heavy metals can then be taken up by plants. From plants a subsequent accumulation through the food chain occurs, therefore posing danger to all trophic levels.[9] This is of exceptional concern because most heavy metals, including lead, have been shown to biomagnify further up in the food web,[15] and unfortunately human beings stand at the top of both terrestrial and aquatic food webs. A visual description and distinction of bioaccumulation versus biomagnification is depicted in **Figure 2.**

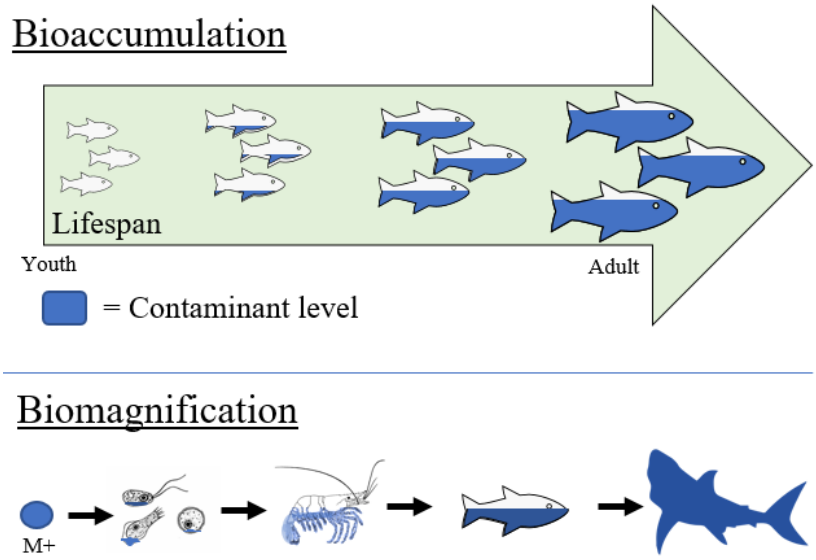

Figure 2: Two ways contaminant level can increase in biological systems.

Detrimental Health Effects from Lead Exposure

When investigating the toxicity concerns of heavy metals on mammalian systems, it has been noted that the toxic effects of heavy metals usually take place within the organ that accumulates the highest concentration of that metal.[16] The toxicity of these metals is largely due to how the metal ions interact within the cellular proteins, enzymes, and cellular membranes. Besides the vast general toxicity of heavy metals, both health and science professionals are becoming more concerned with the potential carcinogenicity of metal compounds, as around 1.7 million new cases of cancer are diagnosed each year in the United States alone.[17]

Lead however, accumulates in a different location than the organs of which its toxic effect takes place. In adults, around 85-95% of lead is stored in bones[18] where it is most-likely mimicking bone calcium. Lead has been found to easily substitute itself for other bivalent cations such as Ca^{2+}, Mg^{2+}, Fe^{2+} and monovalent cations such as Na^{+}, thereby affecting various fundamental biological processes in what is called an ionic mechanism

of lead action[19]. This mechanism has been shown to contribute to neurological deficits. This is largely due to lead's ability to mimic calcium ions, making it possible for lead to cross the blood-brain barrier (BBB) at an appreciable rate. Once lead crosses the BBB, it will start to accumulate in astroglial cells. The effects of lead toxicity are more pronounced in immature astroglial cells, where the nervous system is still developing and is deficient of lead-binding proteins like erthrocytic and plasmatic proteins.[20] This explains why fetuses and young children are most susceptible to neurological damage and behavioral abnormalities caused by lead poisoning. Common health effects from lead poisoning include: ADHD, delayed learning, depression, lethargy, weakness, anemia, elevated blood pressure, hypertension, reproductive problems (i.e. reduced sperm count, decreased libido), renal issues, decreased fetal development, eclampsia, delayed puberty, memory loss, and muscular tremors. With acute toxic exposures (i.e. blood lead levels greater than 0.7 ppm) encephalopathy such as ataxia, comas, convulsions, stupor, and even death can occur.[21]

Current Methods for Heavy-Metal Remediation of Water

Current methods of heavy metal remediation of waste water currently include chemical precipitation, flotation, coagulation and flocculation, membrane filtration, ion exchange, and adsorptive materials like activated carbon.[22] The everyday person is probably most familiar with heavy metal adsorbents like Brita water filters, which contain both activated carbons and ion exchange resins.[23] Ion exchange resins are the most common materials utilized in at-home systems, but as with all technologies ion exchange has some drawbacks. Ion exchange resins require diligent cleaning via backwash and regeneration with brine, and also are very selective to the pH of the effluent.[24]

Metal-Organic Frameworks

The research proposed herein seeks to employ metal-organic frameworks (MOFs) as platforms to adsorb heavy metals from water. MOFs are three-dimensional, crystalline, porous coordination polymers comprised of organic linking units (which are typically either ditopic – ligand forms a complexation at two sites, or tritopic – three sites) and inorganic repeating units often referred to as a node or secondary building unit (SBU). **Figure 3** depicts UiO-66, a three-dimensional MOF that is formed by the coordination between a Zr_6-cluster and terephthalic acid as an example. UiO-66 was first synthesized by Lillerud[25] in 2008 and has since provided a turning point in MOF applications as it was only the second MOF known to remain stable at temperatures past 500°C.[25] It also has been proven to remain stable in aqueous conditions, which is another characteristic lacking in most MOF architectures, as some inorganic nodes are prone to hydrolysis.

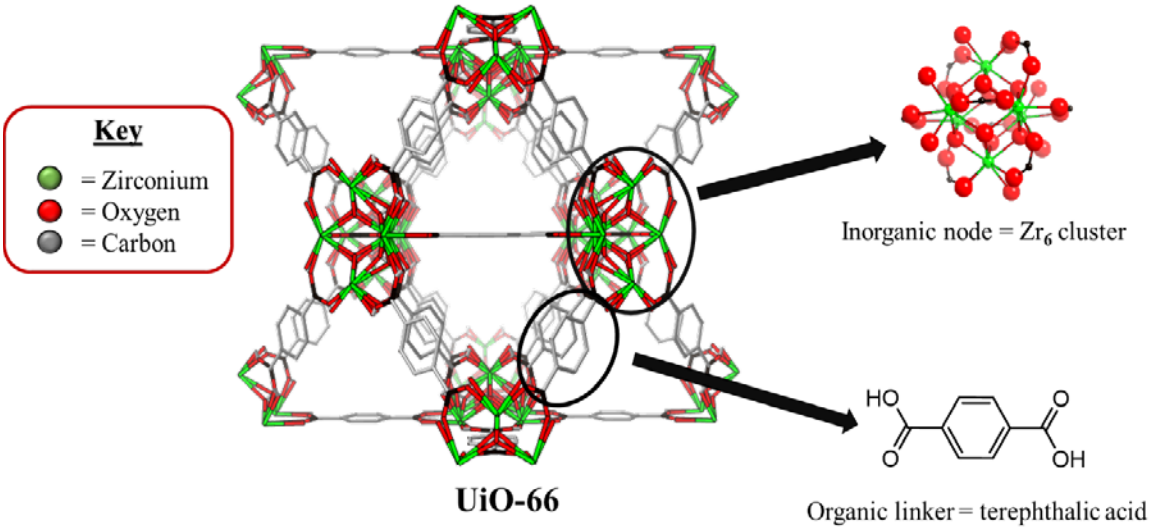

Figure 3: Structure of UiO-66[25]

MOFs are modular in that one could easily vary the constituents' structure, size, and functionality. The unique interchangeability in MOF design of both the node and organic linking unit is one of the driving components in how there has been an exponential

increase in novel MOFs reported and studied since the early 2000s.[26] MOFs have a wide variety of applications due to their ability to house functionality either post-synthetically or by implementing unique and chemically relevant organic linkages. Another benefit of these materials is their large internal surface areas ranging anywhere from 1000 to 10,000 m^2/g, which exceeds those of both zeolites and carbons.[26] By utilizing MOFs large internal surface areas and accessibility to pore space, one could imagine capturing small molecules or contaminants inside. From there the framework could either be recycled or be utilized as a chemical storage vessel. This would prove quite useful when investigating remediating areas contaminated with radioactive metals like cesium or strontium.

Heavy-Metal Adsorption from Water Using MOFs

Although MOFs have been used for applications in adsorption quite extensively, especially for gases like CO_2,[27] using these materials for water purification have only been expounded upon and have shown great advancement in the last ten years. The crucial issue in using MOFs as means of water purification is their instability in water.[28] Therefore, when tackling the issue of water purification using MOFs, the practitioner is limited to only robust and rigid frameworks.

Previous attempts to use MOFs as heavy metal sorbents include either post-synthetic modification/functionalization of the organic linking unit (**Figure 4a)**,[29-32] or by utilizing negatively charged anionic frameworks with natural affinities for metal cations (**Figure 4b)**.[33] Using anionic MOFs would be an attractive route, however compared to the diverse library of MOFs, there are not many water-stable anionic MOFs. Post-synthetic modification of MOFs is attractive, given that the investigated framework can withstand reactions conditions.

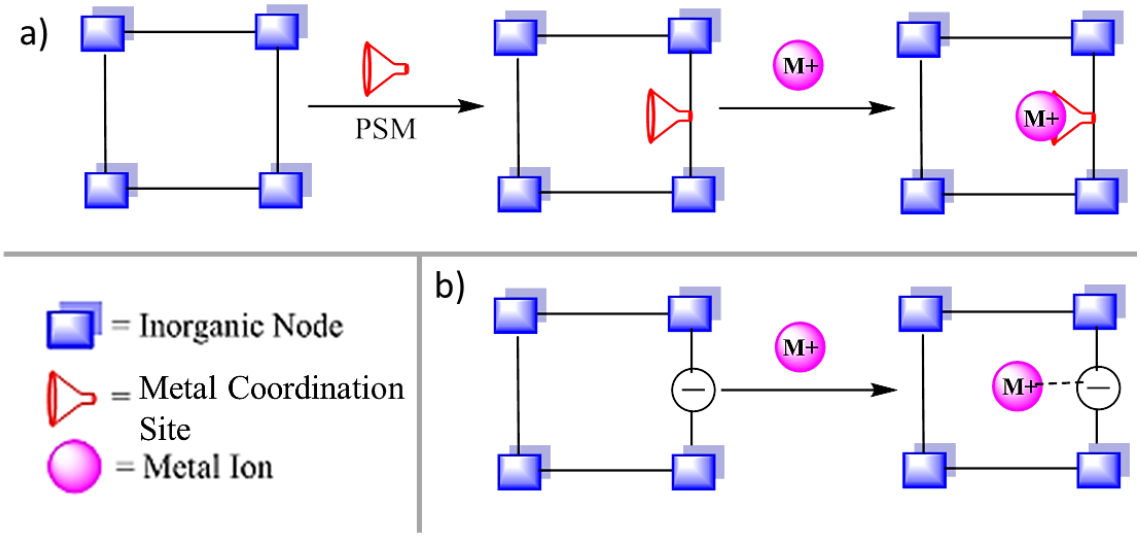

Figure 4: Known methods for heavy metal adsorption in MOFs

In MOF architecture, most organic ligands are comprised of either an aromatic or heterocyclic backbone, owing to many motifs for coordination between heavy metals and the ligand inside of the MOF's porous cavities as depicted in **Figure 5**. Modes of coordination include cation-π, Lewis acid/base interactions, coordination with the node, or simply van der Waals interactions.

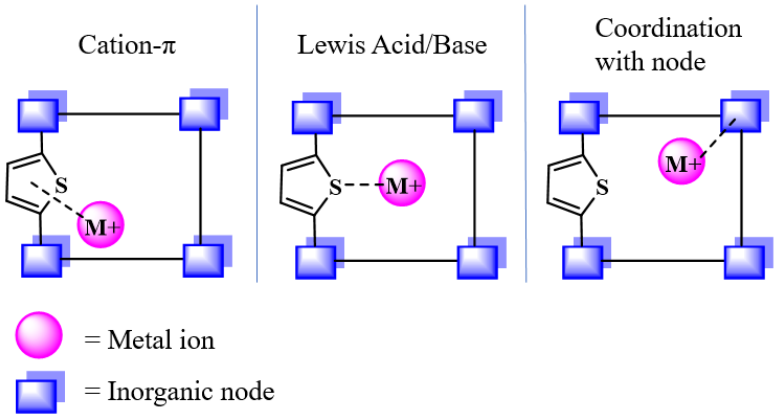

Figure 5: Most common modes of coordination inside of a heterocycle-containing MOF

Thiophenylated-MOFs as Heavy-Metal Sorbants

For this research, organic ligands with a thiophene moiety, as well as inorganic nodes derived from zirconium, have been identified as suitable building blocks for MOF architectures. Zirconium-derived MOFs have been shown to have excellent stability profiles due to the ultra-resilience of the resultant Zr_6 metal cluster.[34-36] Sulfur in general has been shown to excel as a heavy-metal chelator, as it is commonly used in occupational chelation therapy in molecules like dimercaptosuccinic acid (DMSA),[37] which can be administered orally.

The thiophene moiety was selected due to its propensity to bind metals/cations in a variety of ways. Harris[38] was able to show through the modeling of the electronic structures of η^5- and η^1- thiophene-metal complexes that not only is donation from the HOMO of the thiophene into transition metal important for metal-ligand binding, but that the thiophene's empty π^* orbital (LUMO) also participates by receiving back-donation from the metal (**Figure 6**).

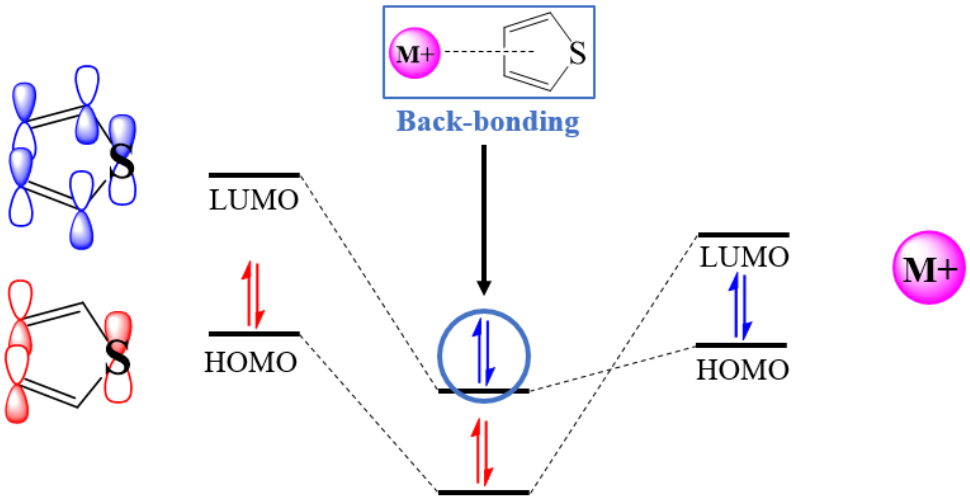

Figure 6: Interaction between the low-lying LUMO of thiophene and The HOMO of the metal ion.

Therefore, π back-donation might even be the most important contributor when thiophene is bound to 4d or 5d metals that exist in a low oxidation state or are electron rich from being coordinated to other strong donor ligands. Whenever π back-donation into the thiophene is maximized, the bonds between carbon and sulfur will begin to weaken,[38] and one could imagine that the changes in C-S bonds could be investigated by using various types of spectroscopy.

Chapter 2: Results and Discussion

Batch Experiments Resulting in MOF Structural Rearrangement

With the thiophene moiety's known metal affinity in mind, we set out to explore metal-organic frameworks containing thiophene. Initial MOFs used in this study were the In-derived ATF-1 (In-derived),[39] and the Cu-derived MOF-107, and MOF-110.[40] These MOFs are depicted in **Figure 7**. ATF-1 was presumed to be an excellent candidate for aqueous lead removal due to its 2,5-thiophenedicarboxylic acid (TDC) linkage and because its framework is negatively charged, it has a natural affinity for cationic species. ATF-1's anionic nature is attributed to its tetrahedral indium SBU, $In(COO^-)_4$.[39] MOF-107 and MOF-110 however are both neutral MOFs comprised of the 2,5-TDC ligand and $Cu_2(COO^-)_4$ paddle wheel.[40]

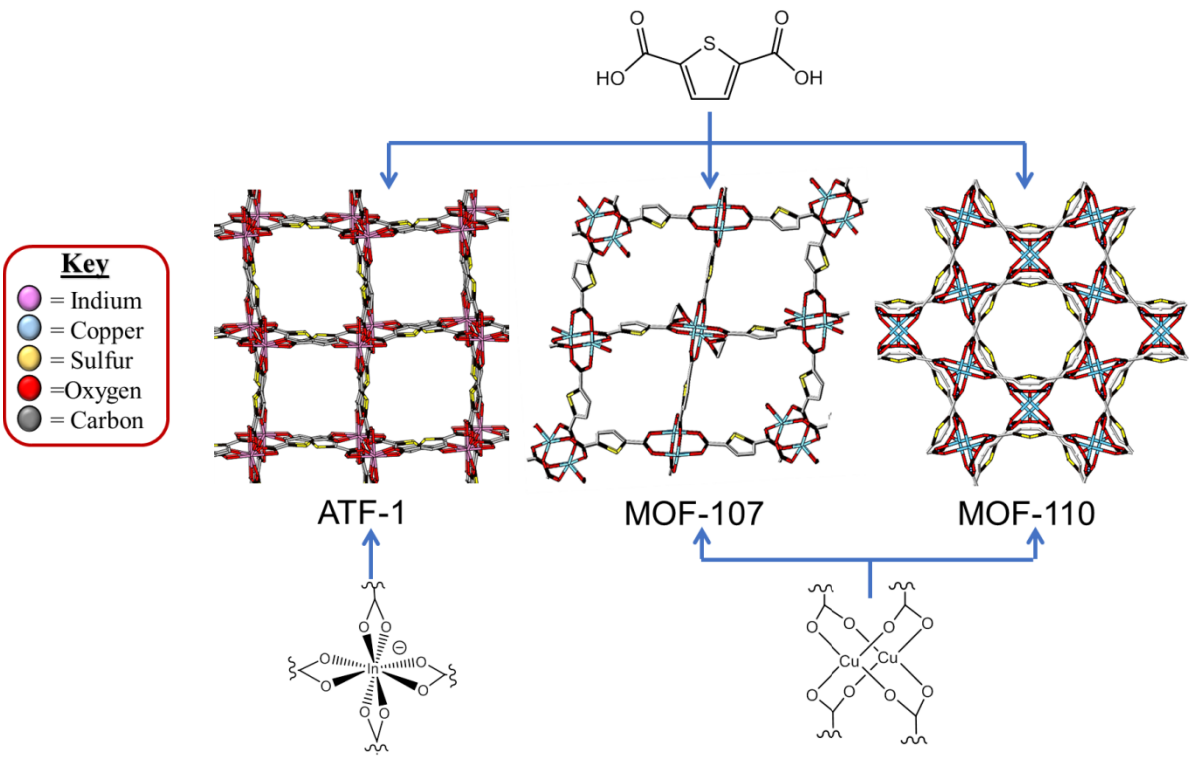

Figure 7: Visual representation of investigated MOFs including ligand and SBU derivatizations.

Initial determination of Pb-affinity of the selected MOFs in **Figure 7** was performed in batch reactions where 20 mg of ground MOF (which was activated prior to use by heating to 100ºC under high vacuum for 2 hours) was added to 3 mL of either a 21 or 2100 ppm aqueous $Pb(NO_3)_2$ solution for 24 hours. At this time an aliquot of solution was removed, diluted, and the resultant concentration of Pb^{2+} ions was observed via inductively-couple plasma mass spectroscopy (ICP-MS) (**Figure 8**).

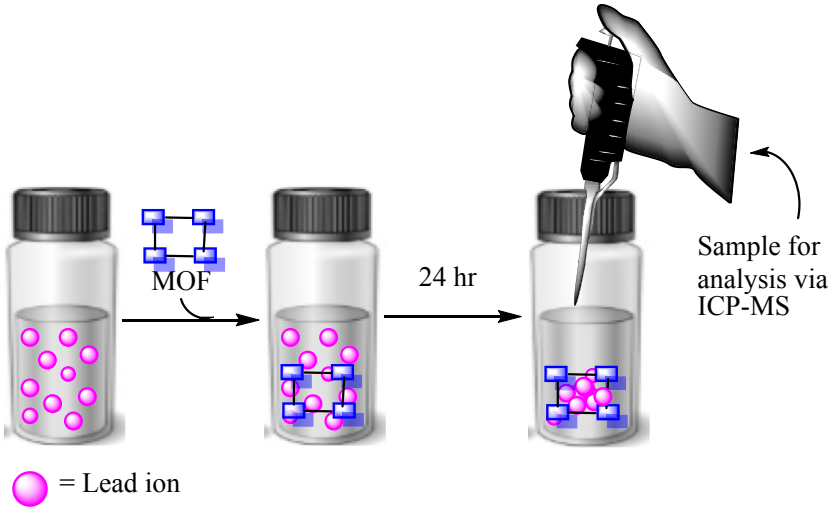

Figure 8: Experimental design for studying lead adsorption in batch reactions

It was observed via ICP-MS that for all three MOFs, the moles of Pb^{2+} adsorbed into each requisite MOF was equal to the calculated mols of metal (indium or copper) leeched into the experimental lead solution at 2100 ppm Pb^{2+}. This implies a metal-displacement phenomenon within each MOF at the inorganic node **Figure 9**.

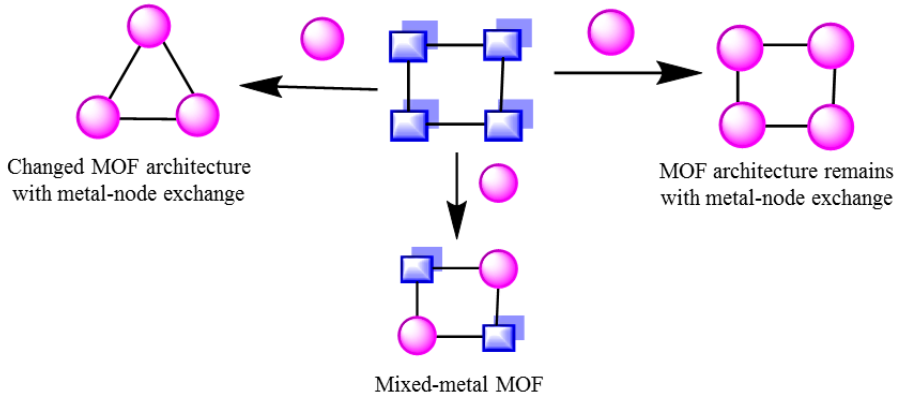

Figure 9. Different modes of metal-displacement in MOFs

PXRD analysis of MOFs confirmed that at high concentration of lead ions (2100 ppm) the MOFs had exchanged the metal at their respective nodes and transformed into new MOFs which were nonisostructural to their predecessors. Through single-crystal analysis it was observed that ATF-1 had transformed into a novel one-dimensional Pb-MOF (**Figure 10**).

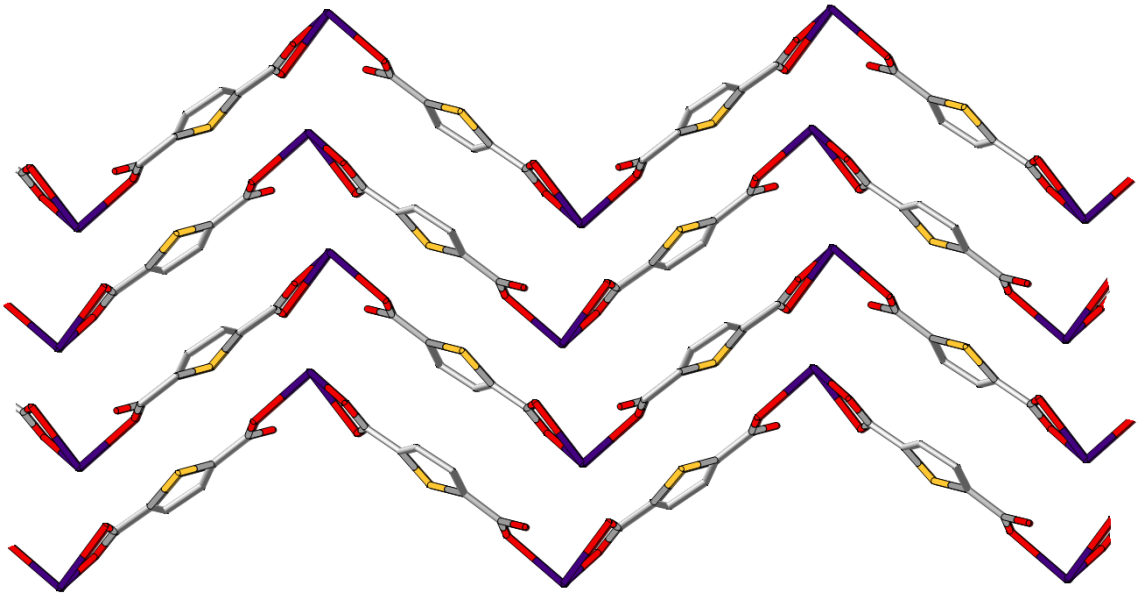

Figure 10. Solved crystal structure for the one-dimensional lead-MOF obtained from subjecting ATF-1 to 2100 ppm Pb^{2+} for 24 hours

It was determined via PXRD that MOF-107 and MOF-110, although different MOFs entirely, had formed the same new lead structure. Visually the copper-derived MOFs, MOF-107 and MOF-110 had lost their blue color within 5 minutes of soaking in the 2100 ppm Pb^{2+} solution (**Figure 11**). The structure of this new Pb-containing material is yet unsolved.

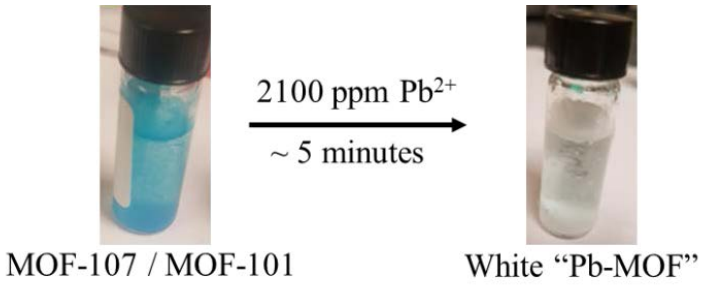

Figure 11. Visual copper-lead displacement in MOFs 107&110

After comparing the bond-dissociation energies (BDEs) of In-O, Cu-O, and Pb-O (**Table 1**)[41], it is not surprising that metal-exchange had occurred. The lead-oxygen bond is much stronger in comparison to the indium-oxygen and copper-oxygen bonds in the initial MOFs, so the resulting formation of the lead-oxygen bonds in the new MOF architectures is thermodynamically favorable. It was observed that at low concentration (21 ppm Pb^{2+}), the MOFs appeared to decompose entirely, most likely through a simple hydrolysis mechanism and not a Pb-Cu/In exchange. These data indicate that these MOFs are not water-stable and are therefore inadequate for water-remediation studies.

Table 1: Reported bond dissociation energies[41] for M-O Bonds related to MOFs in this study

Type of Bond	BDE (kJ/mol)
In-O	320
Cu-O	269
Pb-O	382

Batch Experiments Using Zr-MOFs

With the water-stability of our initial MOFs being an issue, Zr-MOFs became an attractive system due to their unprecedented stability in aqueous environments. This is owed to the ultra-resilience of the inorganic building unit, the Zr_6 cluster. By studying different Zr-MOFs, the practitioner can then best hone-in on systems/architectures most appropriate for the heavy-metal remediation of water. The initial Zr-MOFs tested are shown in **Figure 12**.

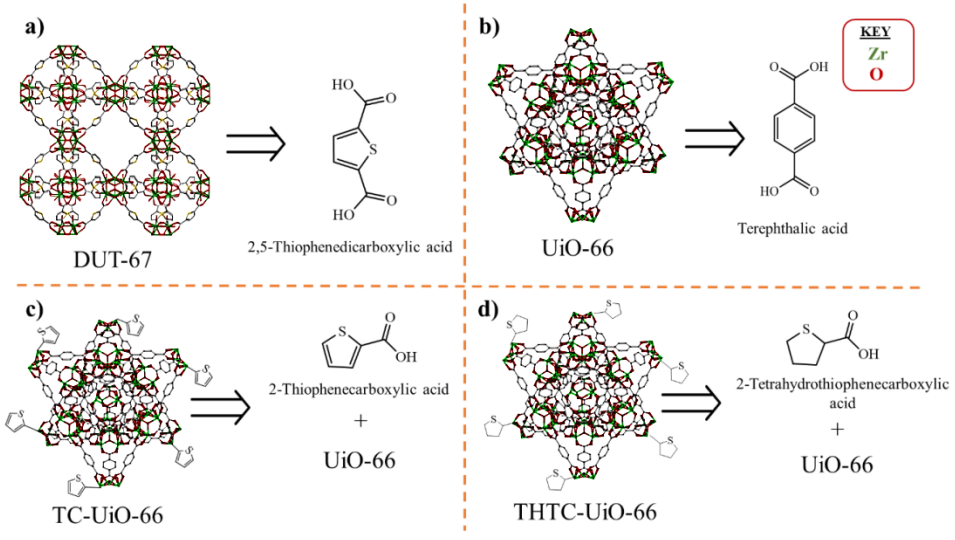

Figure 12: Initial zirconium MOFs screened in lead-adsorptive studies, and their respective derivations as a visual aid.

Figure 12a displays DUT-67 which was first synthesized by Kaskel[42] in two different variations: zirconium and hafnium. DUT-67 (Zr) is an excellent candidate for this study because not only does it contain the ultra-water stable Zr_6 node much like Lillerud's UiO-66[25] (**12b**), but it also contains a thiophene moiety embedded within its ligand. UiO-66 was chosen due to its lack of thiophene-functionality, and could therefore serve as an experimental control. UiO-66 was also interesting because it is known to have defect sites discerning the coordination sites on individual Zr_6 clusters.[42] In UiO-66's crystal structure, each Zr metal center is occupied by 12 organic linkers, and it has been shown by Zhou that UiO-66 actually has a concentration of missing linker defects of up to 10%.[42] These missing linker defect sites are typically occupied by residual solvent molecules which may be displaced post-synthetically by other molecules. This concept inspired us to post-synthetically modify UiO-66 by doping it with 2-thiophenecarboxlic acid (TC, **12c**) and 2-tetrahydrothiophenecarboxylic acid (THTC, **12d**) in hopes to increase its affinity for lead ions. It is important to compare the two variations of post-synthetically modified UiO-66. Thiophene has potential to bind lead through both η^5- and η^1- motifs whereas the tetrahydrothiophene is only left to bind through a Lewis-basic interaction (η^1). One could imagine that with more motifs of binding, as such with thiophene, there would exist a natural higher affinity for lead than with solely η^1- type interactions, not to mention the metals ability to back-donate into thiophene's LUMO, as discussed previously.

All four zirconium MOFs were subjected to either a 2100, 210, or 21 ppm aqueous $Pb(NO_3)_2$ solution under batch conditions to test the MOFs initial affinity for Pb^{2+} ions. After 24 hours, the concentration of Pb^{2+} was analyzed via analytical sampling and subsequent dilutions to a level appropriate for ICP-MS detection. This experiment was

done in triplicate in order to calculate standard errors. The results collected are shown in **Figure 13**.

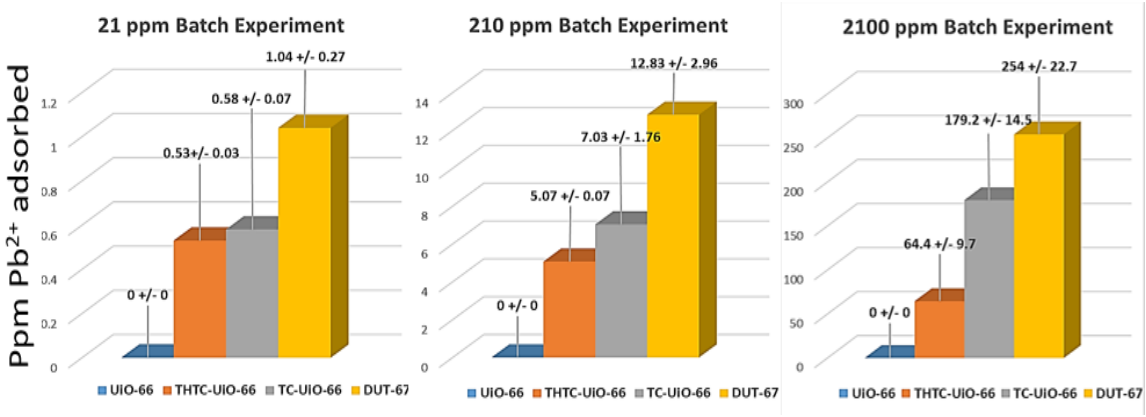

Figure 13: Observed lead adsorption in batch experiments at varying Pb^{2+} concentrations

The data from our initial batch experiments was regarded as strong evidence that the thiophene moiety plays a crucial role in the lead-sorption mechanism in the MOFs studied. DUT-67, which contains thiophene incorporation within its ligand, had adsorbed significantly more lead than the other MOFs at all concentrations. TC-UiO-66 had outcompeted THTC-UiO-66 at all concentrations of lead, which also supports our hypothesis that pi-coordination plays a larger role in lead-binding then sigma-donation alone. Nonfunctionalized UiO-66did not adsorb any lead. In fact, upon sampling the lead solution after UiO-66 had remained within it for 24 hours it was observed via ICP-MS that the concentration of lead in the solution would increase slightly. It is my hypothesis that UiO-66 has a higher affinity for water within the framework, and selectively adsorbs water over lead ions. This was deemed a feasible explanation because the amount of water needed to diffuse into UiO-66 in order to increase the solution concentration by the magnitude observed, could easily be accommodated within UiO-66's interstitial void volume.

Flow Experiments Using Zr-MOFs

After our batch results, we decided to advance lead-adsorption studies by investigating lead-adsorption in flow to see if the selected MOFs could have a more practical use (i.e. at-home water filtration). To this end, we engineered a flow system as shown in **Figure 14**. The experiment takes place at a rate of 0.5mL/minute, with a 1 cm^3 column (internal volume), therefore after every two minutes a column volume of eluent has flown through the MOF. Water samples were collected every column volume for ICP-MS analysis.

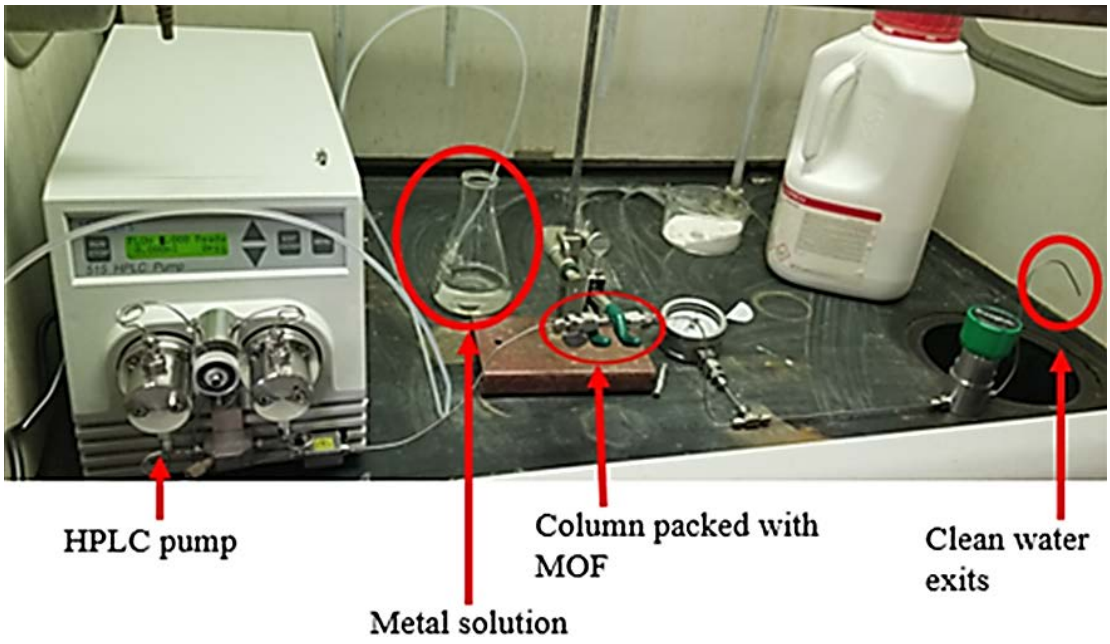

Figure 14: The flow apparatus

Firstly, the flow experiment was conducted with a 2100 ppm aqueous $Pb(NO_3)_2$ solution using UiO-66, TC-UiO-66 and DUT-67. At such high concentration of lead, lead-sorption had occurred in all three MOFs. Testing lead adsorption in MOFs in flow is a useful tool because the MOF in question is constantly being bathed by a fresh lead solution and never allowed to reach equilibrium until saturation. By integrating the area under each

MOFs breakthrough curve (**Figure 15**) and subtracting that area from the rectangular area under the initial concentration line, the amount of lead adsorbed in each MOF could be calculated. Since each breakthrough curve could not accurately be fitted with a best fit line, the Midpoint Rectangle Rule (**Equation 1**) was employed to best approximate the area under the breakthrough curves. By using this method, the area under a breakthrough curve (M_n) between a and b can be approximated by summing midpoint rectangles. The more rectangles derived from data points on any given graph, the better the estimate. The Midpoint Rectangle Rule is displayed below:

$$M_n = \frac{b-a}{n}\left[h_1\left(\frac{x_0+x_1}{2}\right)+h_2\left(\frac{x_1+x_2}{2}\right)+h_3\left(\frac{x_2+x_3}{2}\right)+\cdots+h_n\left(\frac{x_{n-1}+x_n}{2}\right)\right] \quad (\mathbf{1})$$

Where n is the number of rectangles, $\frac{b-a}{n}$ is the width of each rectangle, and h is the heights of the rectangles.

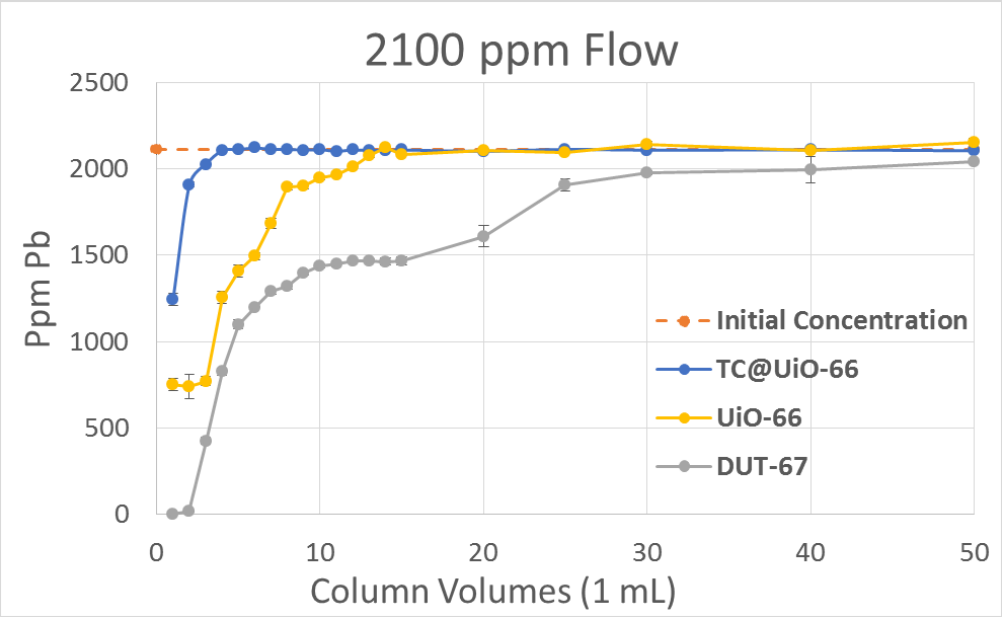

Figure 15: 2100 ppm Pb^{2+} Breakthrough Curve for the Zr-MOFs Under Investigation

DUT-67 had adsorbed the most lead in flow at 2100 ppm Pb^{2+}, followed by UiO-66, with the thiophene-incorporated UiO-66 (TC-UiO-66) adsorbing the least amount of lead. It

seems perplexing at first that the TC-UiO-66 would adsorb the least amount of lead but when you consider the mechanism of thiophene incorporation being at the defect sites of the node, and the fact that these coordinative defect sites are most encounterable on the surface of the MOF, one could argue that lead is binding and occupying the outmost pores of the MOF, therefore potentially blocking access to the inner-most pores. This would not be expected to occur in DUT-67 because not only does it contain two different types of pores, it also has a large channel within its structure that lead ions could travel through until they encounter an uncoordinated thiophene ligand. Once the MOFs were saturated with lead in flow with 2100 ppm Pb^{2+}, they were digested for ICP-MS analysis to calculate their respective mass amounts of lead and zirconium. The amount of lead adsorbed which was calculated by integration can then be compared to the amount of lead observed via ICP-MS analysis of the digested MOFs after lead-exposure (**Table 2**).

After testing the MOFs in a flow application with 2100 ppm Pb^{2+}, we attempted the same experiment except at a more relevant concentration such as an emergency resulting from pipe corrosion like in the Flint Michigan water crisis.[12] Results from the flow experiment at 21 ppm aqueous $Pb(NO_3)_2$ are shown below in **Figure 16**.

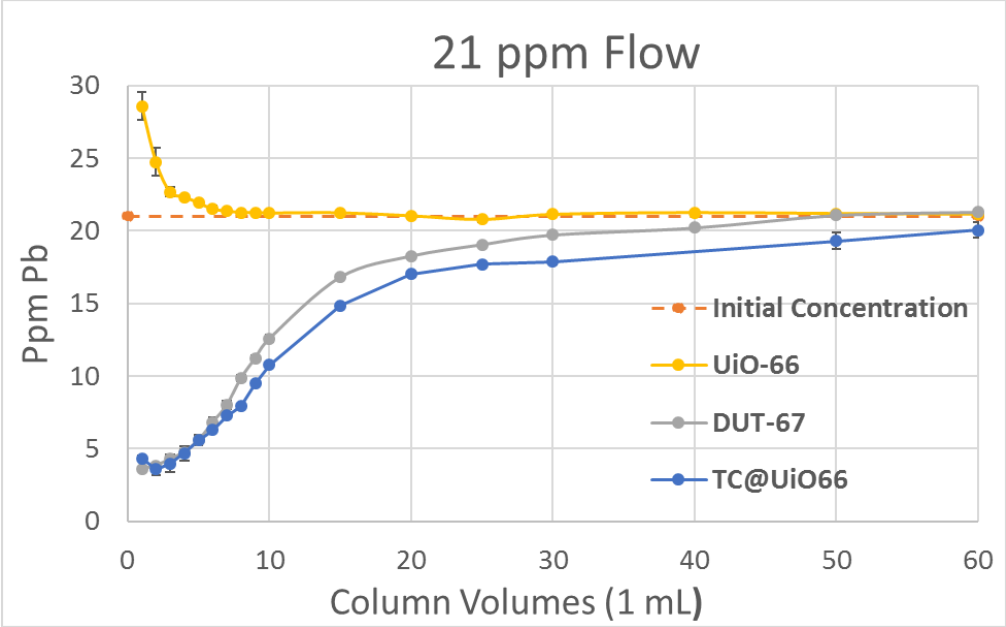

Figure 16: 21 ppm Pb^{2+} breakthrough curve for the Zr-MOFs under investigation

The only MOF with no thiophene-incorporation, UiO-66, had again displayed no lead adsorption. At 21 ppm aqueous $Pb(NO_3)_2$, once more selectively adsorbed water over lead ions within the first five column volumes. It is possible that this was not observed at 2100 ppm aqueous $Pb(NO_3)_2$ owing to physiosorption at such a high concentration of lead ions, but under more dilute conditions, physiosorption does not occur. DUT-67 and TC-UiO-66, the thiophene-containing MOFs had both adsorbed a similar amount of lead at this lowered concentration, supporting that thiophene has the capability to bind lead ions.

Table 2: Amount Pb adsorbed / g MOF - calculated both by integration and ICP-MS of the digested MOFs (post-flow)

	DUT-67		TC-UiO-66		UiO-66	
Calculation Method:	**Integration**	**ICP-MS**	**Integration**	**ICP-MS**	**Integration**	**ICP-MS**
21 ppm Pb^{2+} Flow Experiment	0.96 mg Pb / g MOF	0.93 mg Pb / g MOF	1.27 mg Pb / g MOF	1.22 mg Pb / g MOF	0 mg Pb / g MOF	0.01 mg Pb / g MOF
2100 ppm Pb^{2+} Flow Experiment	98.6 mg Pb / g MOF	100.1 mg Pb / g MOF	8.60 mg Pb / g MOF	8.71 mg Pb / g MOF	26.8 mg Pb / g MOF	23.2 mg Pb / g MOF

Recyclability of DUT-67 in Flow

It was promising that the thiophene-containing MOFs had shown the capability to adsorb Pb^{2+} ions in water, but it then became pertinent to know whether or not the MOFs could be recycled. DUT-67 was selected because it did not have to undergo any type of post-synthetic modification in order to incorporate thiophene, and is also less defective than the UiO-66 derivatives. **Figure 17** displays DUT-67 after being subjected to 21 ppm aqueous $Pb(NO_3)_2$ five times. Ethanol was used to regenerate the MOF in between runs by simply flowing it through the column. DUT-67 had displayed excellent recyclability, with only a minor loss in activity.

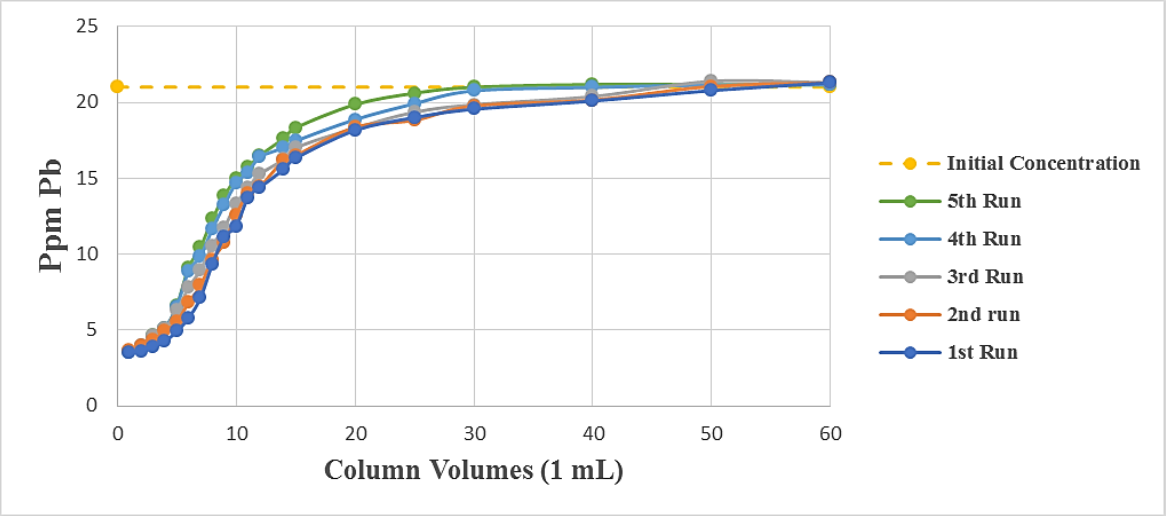

Figure 17: 21 ppm Pb2+ Breakthrough Curve for Recycled DUT-67 after 5 Runs

Solution-State Lead NMR Experiments

Following batch and flow experiments, ^{207}Pb nuclear magnetic resonance spectroscopy (NMR) was employed in order to observe any lead-thiophene interactions. Solid-state NMR (SS NMR) of the spent-MOFs would be an attractive route, but SS NMR is not always accessible or informative. Therefore solution-phase NMR studies were conducted by dissolving $Pb(NO_3)_2$ in deuterated DMSO and adding increased amounts of either thiophene or tetrahydrothiophene into the experimental solution. Coaxial NMR tube inserts (**Figure 18**) contained a $Pb(NO_3)_2$ standard were also used. This allowed to observe any shifting of the $Pb(NO_3)_2$ peak, following the addition of requisite heterocycle.

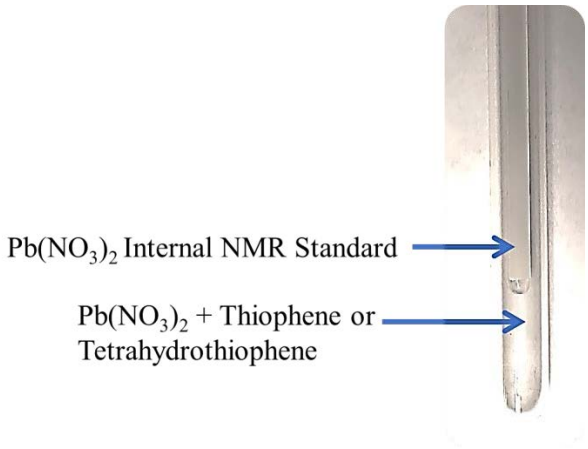

Figure 18: NMR sample tube containing a $Pb(NO_3)_2$ standard within the coaxial insert tube for visual aid

Via the use of ^{207}Pb NMR, chemical shifting of the $Pb(NO_3)_2$ peak was observed upon the addition of one and two equivalents of both thiophene and tetrahydrothiophene. These shifts are listed below in **Table 3**.

Table 3: Shifting of the $Pb(NO_3)_2$ peak after the addition of heterocycle

Equivalents heterocycle	Shift from $Pb(NO_3)_2$ – Thiophene	Shift from $Pb(NO_3)_2$ – Tetrahydrothiophene
1	-6.88 ppm	-8.02 ppm
2	-18.59 ppm	-5.61 ppm

It was reported by Jutzi and Burford[44] that π-cyclopentadienyl bound metal complexes (for metals with NMR active nuclei) result in a distinctive upfield chemical shift, which can be rationalized in terms of ring current phenomena.[45-48] Metals within sandwich complexes in particular, experience significant upfield chemical shifts due to their "double shielding" by two aromatic molecules.[46,48] Therefore the extremely large shift upon the addition of two equivalents of thiophene (-18.59 ppm) can be indicative of a

plumbacene-type interaction, once more providing support that lead has the propensity to coordinate to thiophene via an η^5-binding motif. The shift experienced by the addition of tetrahydrothiophene is owed to electron donation from the sulfur atom to lead. The mode of coordination between one equivalent of thiophene however cannot be identified as η^1- or η^5- since it is much too close to the shifts experienced by tetrahydrothiophene.

Proposed Mechanism of Lead Adsorption in DUT-67

After confirming that DUT-67 adsorbs 98.6 mg of Pb / g DUT-67 at 2100 ppm Pb^{2+}, we realized that implies there is exactly two lead ions in each pore of DUT-67. This would help explain why in DUT-67's 2100 ppm Pb^{2+} breakthrough curve was differently shaped then every other curve generated. The shape of a breakthrough curve is indicative of the mechanism of mass transfer from the eluent to the adsorbent.

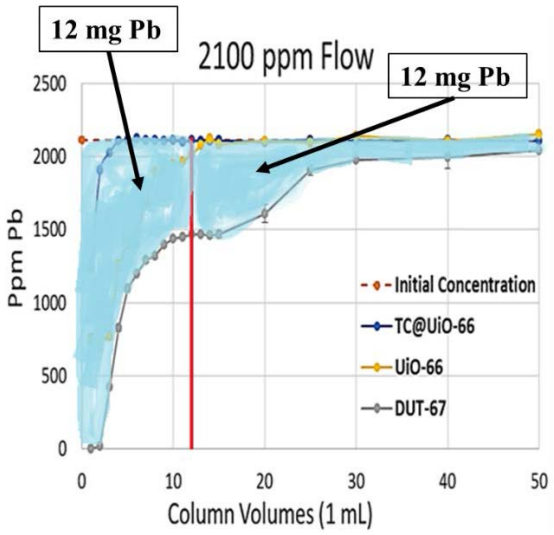

Figure 19: Integrating the amount of lead (mg) in DUT-67

After about 13 column volumes, DUT-67's breakthrough curve plateaus before it increases once more (**Figure 19**). When this curve is divided into two individual sections and the amount of lead is integrated for each section, it was found that the amount of lead in each section where equal. We hypothesize that during the first curve, the first lead ion is

deposited and bound inside each pore, and the second lead ion then with start filling the already-once-occupied pores during the second curve. When modeled in Crystal Maker™ software (**Figure 20**), we found that each lead ion most likely sits in between two thiophene molecules, and due to charge repulsion, each lead ion sits in adjacent sides of each pore.

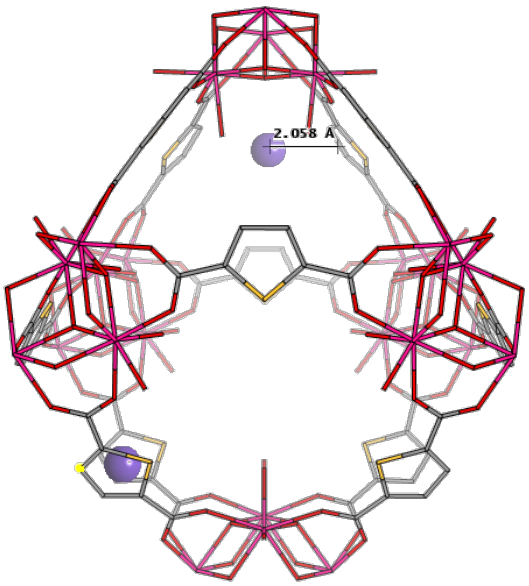

Figure 20: Model of the lead ions inside of one pore of DUT-67

The placement of the lead ion between two thiophenes once again proposes a plumbacene-type interaction. When modeled the lead-thiophene distance is 2.058 Å, which can be compared to the sandwich complex ferrocene[49], with an iron-Cp distance of 2.04 Å. This once again support strong evidence of η^5-interactions between lead and thiophene.

Conclusions

The work within this thesis supports that the incorporation of a thiophene moiety into a MOFs architecture increases it's affinity for lead ions in aqueous media. It was proven that MOFs which contain thiophene (TC-UiO-66, DUT-67), have the propensity to bind lead ions over MOFs with no functionality (UiO-66). The mechanism of binding is hypothesized to be the formation of a lead-thiophene sandwich complex. This is heavily

supported through ^{207}Pb NMR analysis, integration of the DUT-67 breakthrough curve at 2100 ppm Pb^{2+}, and molecular modeling of the lead ion within the pore of DUT-67. To our knowledge, there exists no support for a lead-thiophene sandwich complex in literature until this work was completed.

Chapter 3: Experimental

Synthesis of ATF-1

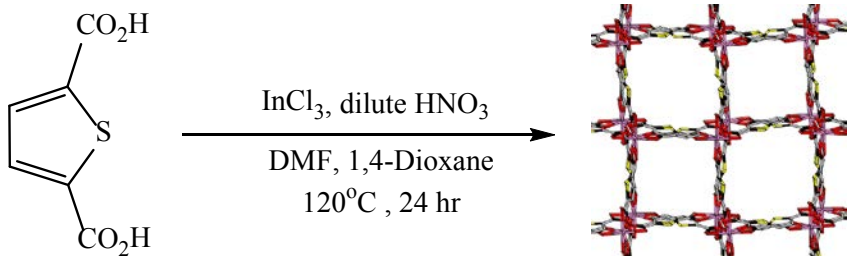

To a premixed solution of DMF (18 mL) and dioxane (12 mL) was added 2,5-thiophenedicarboxylic acid (107 mg, 0.620 mmol, 1.00 eq.) and $InCl_3$ (291 mg, 1.32 mmol, 2.13 eq.). To the resultant homogenous solution was added a separate premixed solution of concentrated nitric acid (0.025 mL) and deionized water (2 mL) and the resulting mixture was subjected to sonication for 10 minutes. The resulting homogeneous solution was then filtered through a GE 25 mm PVDF syringe filter (0.45 μm) in 6 mL portions into individual 20 mL scintillating vials. The vials were then sealed with Teflon-lined caps and subjected to heating in a 120 °C oven for 24 hours. The vials were then removed and set aside to cool at ambient temperature. Crystals from each individual vial were combined and washed 3x with 10 mL fresh DMF each time before drying the afforded crystalline product on a schlenk line under high vacuum at ambient temperature overnight. At this time the crystals were then activated by drying *in vacuo* at 100 °C. Crystal samples were then thoroughly ground before use to assure a homogeneous representation of crystallites. Powder X-ray diffraction data matched that as previously reported.[39]

Synthesis of MOF-107

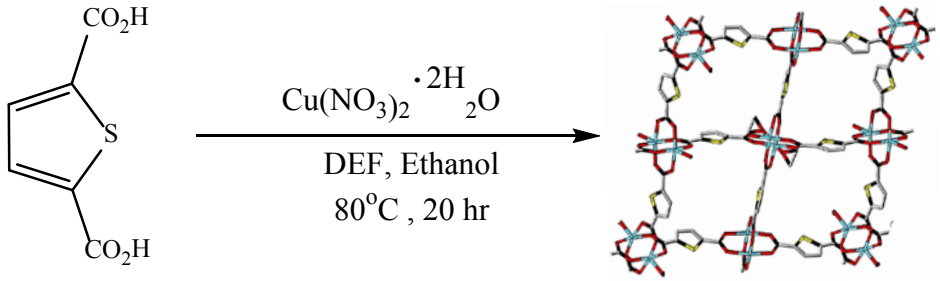

To a premixed solution of DEF (16 mL) and ethanol (4 mL) was added 2,5-thiophenedicarboxylic acid (180.0 mg, 0.100 mmol, 1.00 eq.) and copper(II) nitrate hemipentahydrate, (235.0 mg, 0.100 mmol, 1.00 eq.) and the resulting mixture was subjected to sonication for 10 minutes. The resulting homogeneous solution was then filtered through a GE 25 mm PVDF syringe filter (0.45 μm) in 4 mL portions into individual 20 mL scintillating vials. The vials were then sealed with Teflon-lined caps and subjected to heating in a 80°C oven for 20 hours. The vials were then removed and set aside to cool at ambient temperature. Crystals from each individual vial were combined and washed 3x with 10 mL of the DEF/ethanol mixture each time before drying the afforded crystalline product on a schlenk line under high vacuum at ambient temperature overnight. At this time the crystals were then activated by drying *in vacuo* at 100°C. Crystal samples were then thoroughly ground before use to assure a homogeneous representation of crystallites. Powder X-ray diffraction data matched that as previously reported.[40]

Synthesis of MOF-110

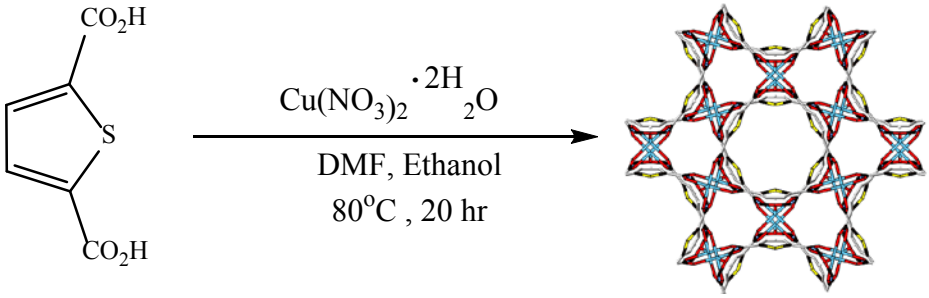

To a premixed solution of DMF (15 mL) and ethanol (5 mL) was added 2,5-thiophenedicarboxylic acid (180.0 mg, 0.100 mmol, 1.00 eq.) and copper(II) nitrate hemipentahydrate, (235.0 mg, 0.100 mmol, 1.00 eq.) and the resulting mixture was subjected to sonication for 10 minutes. The resulting homogeneous solution was then filtered through a GE 25 mm PVDF syringe filter (0.45 μm) in 4 mL portions into individual 20 mL scintillating vials. The vials were then sealed with Teflon-lined caps and subjected to heating in a 80°C oven for 20 hours. The vials were then removed and set aside to cool at ambient temperature. Crystals from each individual vial were combined and washed 3x with 10 mL of the DEF/ethanol mixture each time before drying the afforded crystalline product on a schlenk line under high vacuum at ambient temperature overnight. At this time the crystals were then activated by drying *in vacuo* at 100°C for 2 hours. Crystal samples were then thoroughly ground before use to assure a homogeneous representation of crystallites. Powder X-ray diffraction data matched that as previously reported.[40]

Synthesis of UiO-66

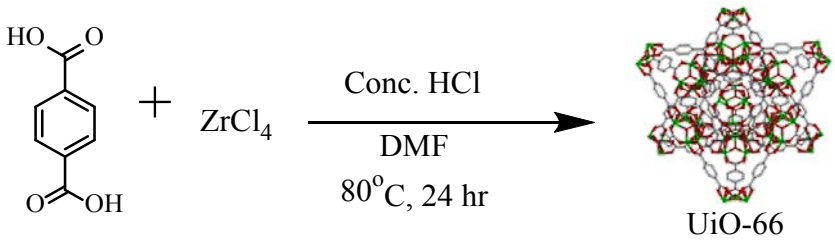

UiO-66

To a 50 mL Erlenmeyer flask loaded with $ZrCl_4$ (250 mg, 1.07 mmol, 1.00 equiv) and DMF (10 mL) was added conc. HCl (2 mL, 20.40 mmol, 19.03 equiv). The resulting solution was sonicated for 20 minutes. In a second 50 mL Erlenmeyer flask, terephthalic acid (246 mg, 1.48 mmol, 1.38 equiv) was dissolved in DMF (20 mL) and sonicated for 10 minutes. The ligand and metal solutions were then combined and sonicated together for an additional 20 minutes. The resulting solution was then filtered through a GE 25 mm PVDF syringe filter (0.45 μm) into 5.3 mL portions into 6 individual 20 mL scintillation vials. The vials were sealed with Teflon-lined caps and heated in an oven at 80°C for 24 hours. At this time, the vials were removed from the oven and cooled to room temperature. The contents of each vial were combined and the combined crystalline powder product was separated from the reaction liquid by centrifugation (5000 rpm for 5 minutes) and washed several times with both DMF and EtOH. The powder was then dried *in vacuo* at ambient temperature for 24 hours. At this time, the powder was activated at 100ºC *in vacuo* for 2 hours. Powder samples were then thoroughly ground before use to assure a homogeneous representation of crystallites. Powder X-ray diffraction data matched that as previously reported.[25]

Synthesis of TC-UiO-66 and THTC-UiO-66

To a 20 mL scintillation vial containing 10 mL of a 1 M solution of the desired dopant (thiophenecarboxylic acid or tetrahydrothiophenecarboxylic acid) in DMF was added 500 mg of ground, activated UiO-66. The vial was then agitated on an orbital shaker (~100 RPM) for 24 hours, after which the powder was analyzed via powder X-ray diffraction and digested for ^{1}H NMR and ^{13}C NMR spectroscopy.

Synthesis of DUT-67

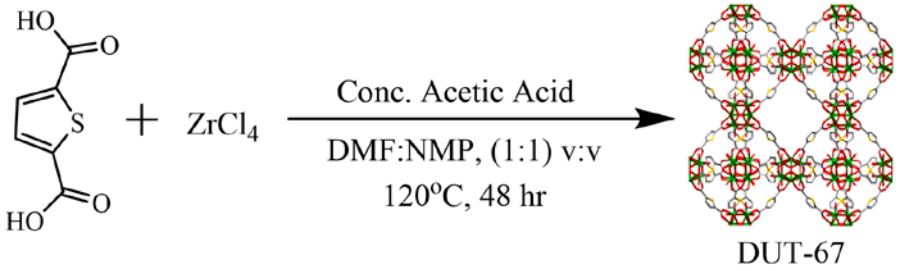

To a premixed solution of DMF (25 mL) and NMP (25 mL) was added $ZrCl_4$ (460 mg, 2.00 mmol, 1.57 equiv). The mixture was then sonicated for 10 minutes until the solution was homogeneous. 2,5-Thiophenedicarboxylic acid (220 mg, 1.27 mmol, 1.00 equiv) was added to the resulting solution, which was then sonicated for 10 minutes. Acetic acid (20 mL, 334 mmol) was then added to the resulting solution, which was then sonicated for an additional 10 minutes. The reaction solution was then filtered through a GE 25 mm PVDF syringe filter (0.45 μm) in 5 mL portions into fourteen individual 20 mL scintillation vials. The vials were sealed with Teflon-lined caps and heated in an oven at 120 °C for 48 hours. At this time, the vials were removed from the oven and cooled to room temperature. The contents of each vial were combined and the combined crystalline powder product was separated from the reaction liquid by centrifugation (5000 rpm for 5 minutes) and then washed several times with both DMF and EtOH. The powder was then dried at room

temperature under high vacuum for 24 hours. At this time, the powder was activated at 100 ^{o}C *in vacuo* for 2 hours. Powder samples were then thoroughly ground before use to assure a homogeneous representation of crystallites. Powder X-ray diffraction data matched that as previously reported.[42]

Aqueous Lead-Removal in Batch Experiments

To a 4 mL screw thread vial was added 20 mg of the requisite MOF followed by 3 mL of either a 21, 210, or 2100 ppm aqueous solution of $Pb(NO_3)_2$. MOFs were left to sit in the Pb^{2+} solution for 24 hrs before aliquots of the solution were taken, diluted, and analyzed using inductively coupled plasma mass spectroscopy (ICP-MS).

Aqueous Lead-Removal in Flow Experiments

Pb^{2+} loading in MOFs was determined by flowing either a 21 or 2100 ppm aqueous solution of $Pb(NO_3)_2$ through a 1 inch stainless steel column (1/4 OD), packed with 250 mg of the requisite MOF*, using a Waters 515 HPLC pump at a flow rate of 0.5 mL/min. Each column volume was fractionated and aliquots were taken of each column (1 mL), diluted, and analyzed using ICP-MS.

*MOFs were first primed with DI water by flowing DI water through the MOFs at a flow rate of 0.5 mL/min for 30 minutes.

Regeneration of DUT-67 in Flow at 21 ppm aqueous $Pb(NO_3)_2$

After exposing DUT-67 to Pb^{2+} adsorption in flow (IIc), DUT-67 was tested for four additional cycles by first eluting 200 proof ethyl alcohol at a flow rate of 0.5 mL/min for 1 hour and then subsequently flowing fresh DI water through the MOF at a flow rate of 0.5 mL/min for 30 minutes. The washed MOF-containing column was then re-exposed to 21 ppm solutions of $Pb(NO_3)_2$ under experimental flow conditions stated previously.

MOF digestion for NMR and ICP-MS Analysis

To 0.66 mL of DMSO-d_6 was added approximately 5 mg of the requisite MOF. To this heterogeneous mixture was added 0.33 mL of concentrated HF before being sonicated as needed until the solution was homogeneous. To this solution was added 0.0511 mmols of ethyl acetate* (5µL) as an internal standard. The resulting solution was analyzed via NMR without further preparation. After collection, the solution was diluted with deionized water for analysis via ICP-MS.

**Note regarding MOF digestion:* Under the acidic conditions of the NMR solution, it was observed via H^1NMR that some of the ethyl acetate had been hydrolyzed to ethanol and acetic acid.

Materials and Methods

I. Reagents and Instrumentation

Acetic acid, thiophene, tetrahydrothiophene, terephthalic acid, zirconium chloride, and D_6-DMSO were purchased from Sigma-Aldrich and used as received. $Pb(NO_3)_2$ and DMF was purchased from Fisher Scientific and used as received. 2,5-Thiophenedicarboxylic acid was purchased from TCI Chemicals and used as received. N-Methyl-2-pyrolidone was purchased from Acros Organics and used as received. 200 proof ethyl alcohol was purchased from Pharmco aaper and used as received.

ICP data were collected on a Thermo Scientific ICAP Qc equipped with a Cetac ASX-520 auto sampler.

NMR data were collected on a 400 MHz Bruker Avance NMR Spectrometer.

II. X-ray Powder Diffraction

Powder XRD patterns of small samples were collected on a Bruker AXS X8 Prospector CCD single crystal diffractometer using the "pilot" plugin for collection of multicrystalline XRD patterns. The instrument is equipped with a copper IμS microsource with a laterally graded multilayer (Goebel) mirror for monochromatization (λ = 1.54178 Å, beam size 0.1-0.2 mm) and an ApexII CCD area detector. Powder samples were thoroughly ground to assure a representative number of crystallites to be present in the X-ray beam. Powder samples were mixed with small amounts of mineral oil and mounted onto a 0.4 mm diameter Mitegen micromesh mount for data collection. Samples were centered in the beam using the instrument's mounting microscope video camera. Data were collected in an emulated theta-2theta setup using the Apex2 software package of Bruker AXS. The sample mount was aligned horizontally (Chi = 0°) and theta angles were set to eight different angles between 12 and 96° to cover a range equivalent to a 0 to 110° range of a powder X-ray diffractometer operated in Debye Scherrer mode (omega angles of each run were set to half the theta values). Samples were rotated around the mount's spindle axis during measurement (360 rotation around phi), typical exposure times were 30 seconds per frame collected. The eight individual patterns taken were corrected for unequal sample to detector surface distance ("unwarped") and were combined into one continuous pattern using the "pilot plugin" software embedded in the Apex2 software package. Data were integrated over 2theta, converted in powder XRD patterns in Bruker "raw" format and were further processed with standard powder XRD software packages.

Supplemental Figures

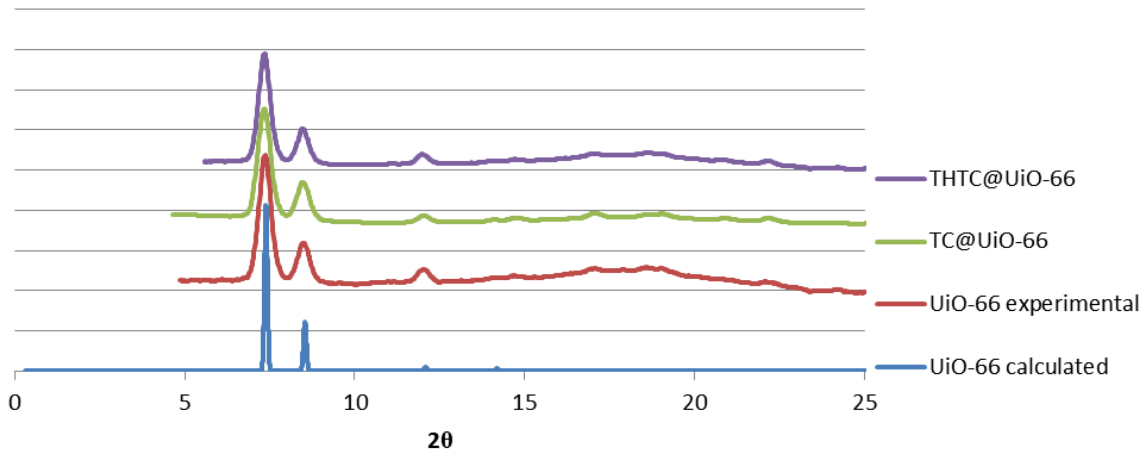

Figure S1: UiO-66 Before and After Post-Modification with TC and THTC

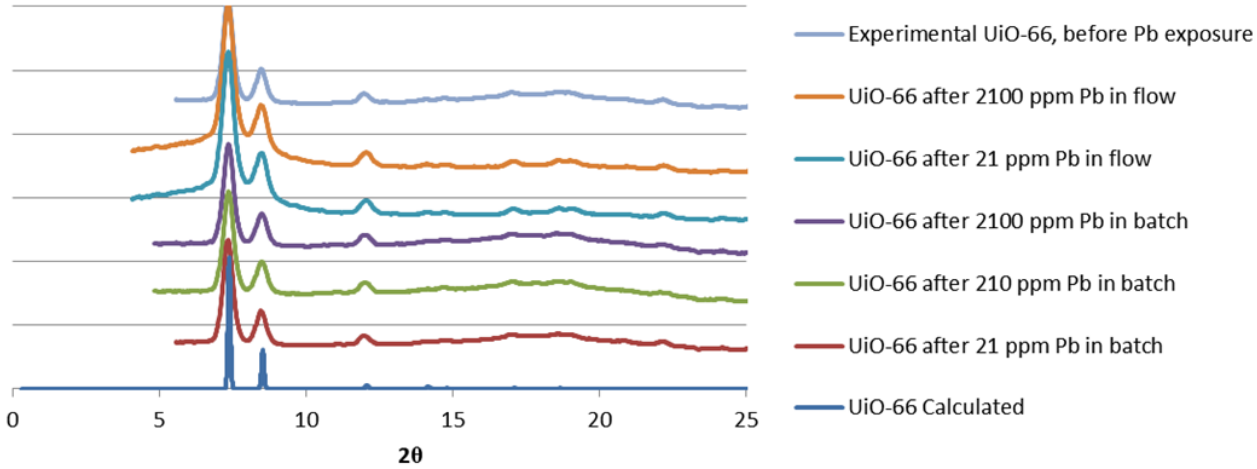

Figure S2: UiO-66's Stability after Batch and Flow Experiments

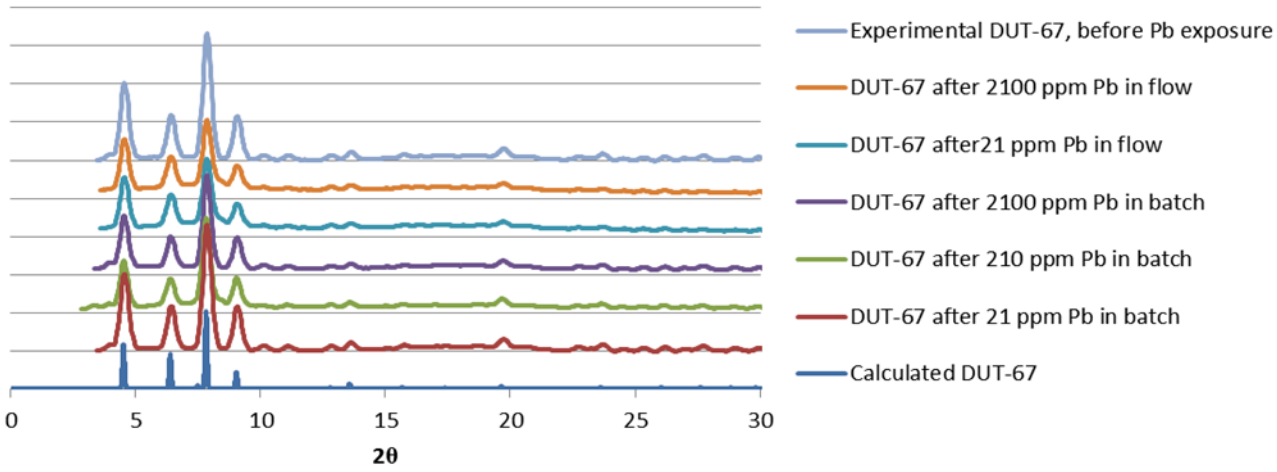

Figure S3: DUT-67's Stability after Batch and Flow Experiments

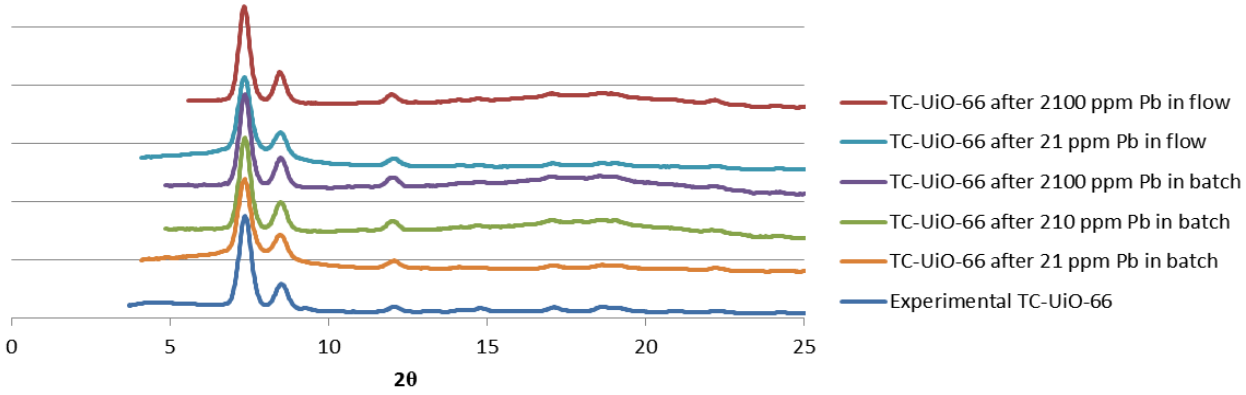

Figure S4: TC-UiO-66's Stability after Batch and Flow Experiments

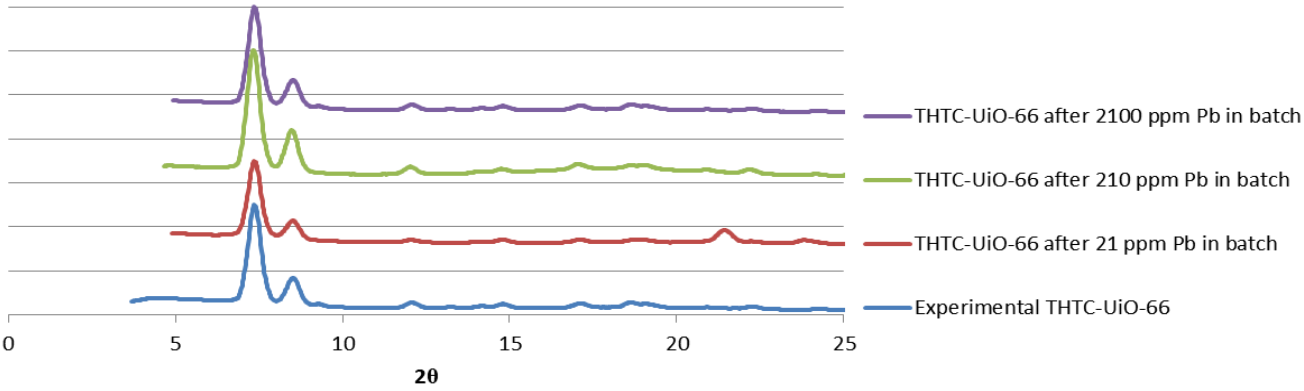

Figure S5: THTC-UiO-66's Stability after Batch and Flow Experiments

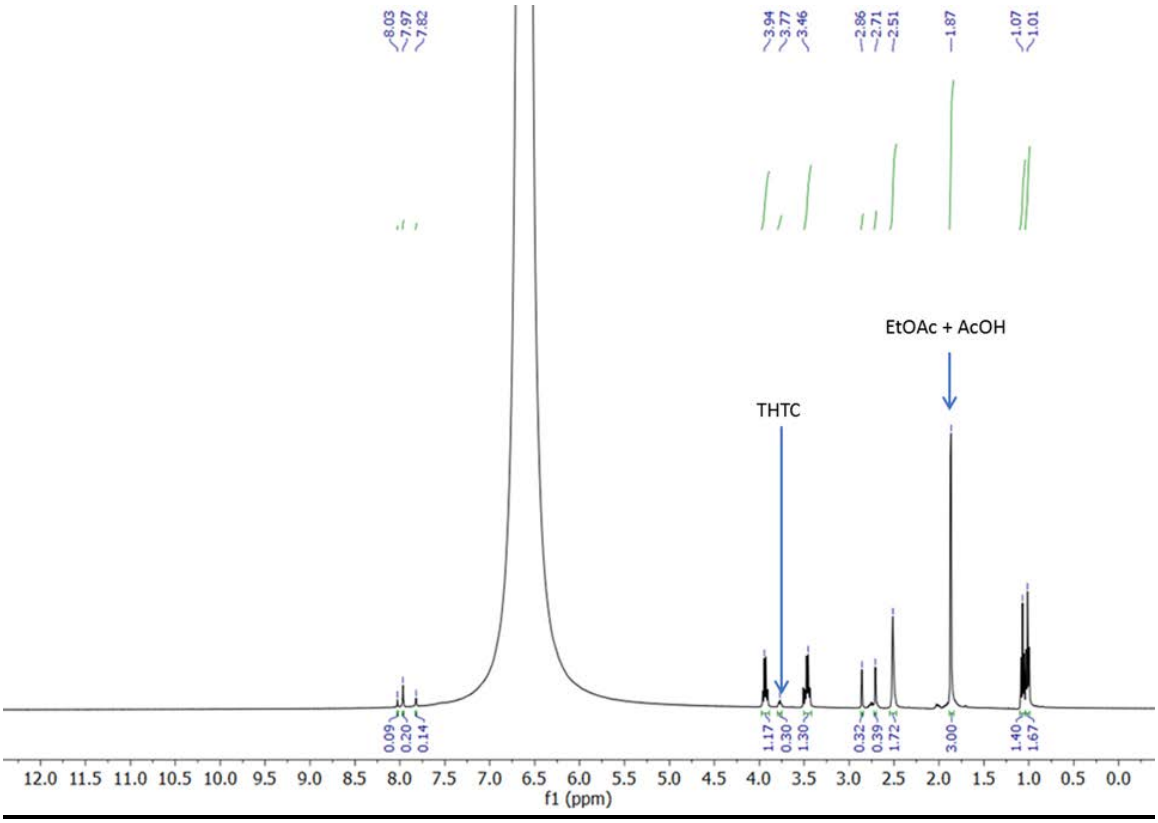

Figure S6: THTC-UiO-66 Proton NMR

To calculate the amount of heterocycle (THTC or TC), the following formula was used:

$$(\ heterocyle\ integral\ value\ from\ NMR) * (mmol\ EtOAc) = \ (mmol\ heterocyle)$$

Where mmol EtOAc = 0.0511

Sample Calculation for **Figure S6**:

$$(0.30\ ) * (0.0511) = 0.0153\ mmol\ THTC$$

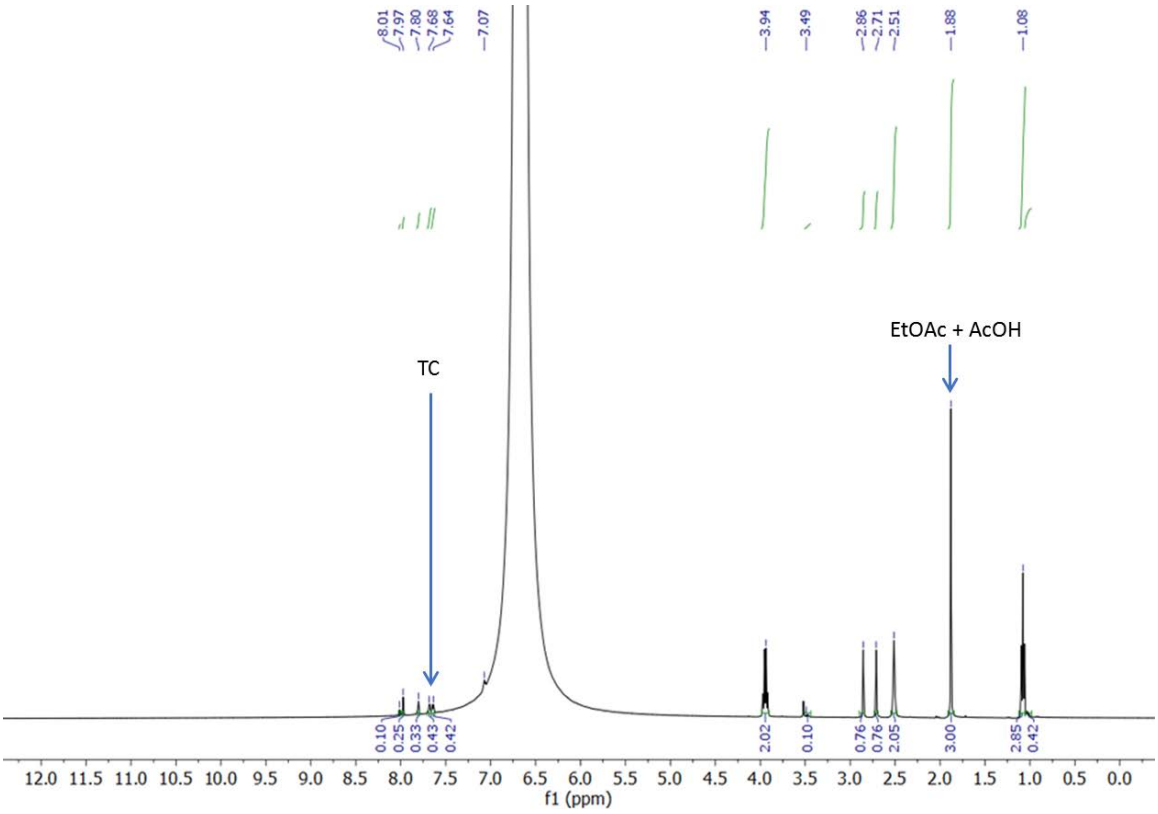

Figure S7: TC-UiO-66 Proton NMR

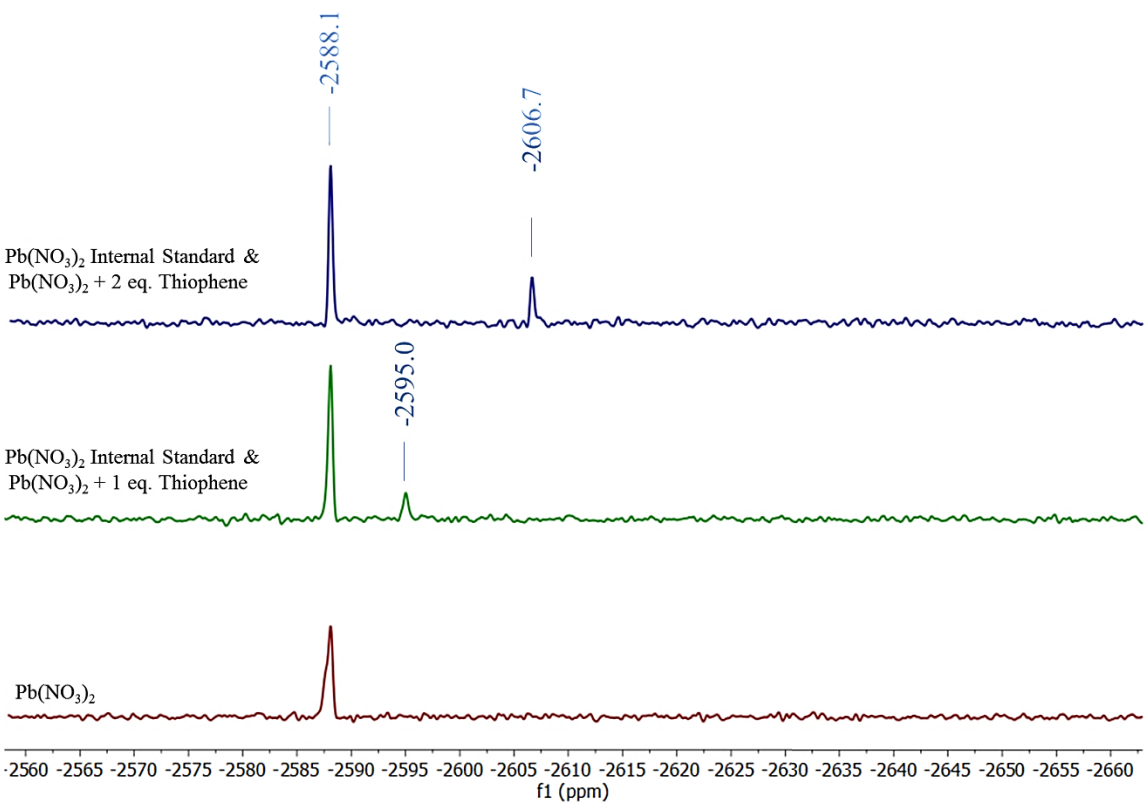

Figure S8: Adding Increasing Equivalents of Thiophene to $Pb(NO_3)_2$

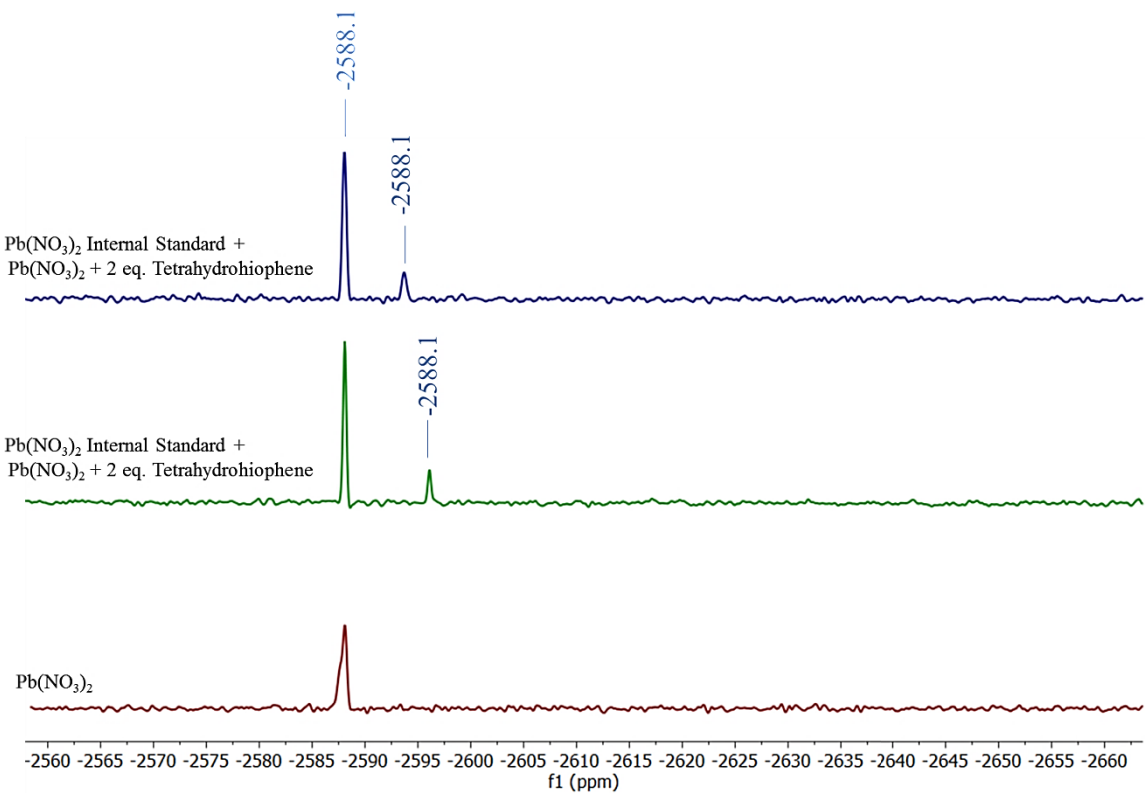

Figure S9: Adding Increasing Equivalents of Tetrahydrothiophene to $Pb(NO_3)_2$

References

1. Li, Y.; Yang, Z.; Cai, H.; Bao, M.; Yu, Y.; Lu, J. "Insight into the highly efficient degradation of PAHs in water over graphene oxide/Ag_3PO_4 composites under visible light irradiation" *Chem. Eng. Journal*., **2018**. 334: 355-376
2. Chalker, J. M.; Hayball, J. D.; Plush, S. E. "Polymer Supported Carbon for Safe and Effective Remediation of PFOA- and PFOS-Contaminated Water" *ACS Sustainable Chem. Eng.,* **2019**. 7(13): 11044-11049
3. Buelna, G.; Tyagi, R. D.; Tiwari, B. "Review on fate and mechanism of removal of pharmaceutical pollutants from wastewater using biological approach" *Bioresource Tech.*, **2017**. 224: 1-12
4. Bharti, Pawan. "Heavy Metals in Environment" *Lambert Academic Publishing,* **2012.**
5. The Water Project, "Facts about Water: Statistics of the Water Crisis". August 31, **2016**. Web. https://thewaterproject.org
6. Corcoram, E.; Nellemann, C.; Baker, E.; Bos, R.; Osborn, D.; Savelli, H. "Sick Water? The Central Role of Wastewater Management in Sustainable Development" *A Rapid Response Assessment by UNEP,* **2010**. Web. www.grida.no
7. History.com Staff, "Water and Air Pollution" *A+E Networks*, **2009**. Web. http://www.history.com/topics/water-and-air-pollution
8. Triplett, G. E.; Han, F. X.; Banin, A.; Su, Y.; Monts, D. L.; Plodinec, J. M.; Kingery, W. L. "Industrial age anthropogenic inputs of heavy metals into the pedosphere" *Naturwissenschaften,* **2002**. 89(11): 497-504
9. Singh, Jiwan. "Effects of Heavy Metals on Soil, Plants, Human Health and Aquatic Life" *IJRCE,* **2011.**
10. Atieh, M.A., Ji, Y., Kochkodan, V. "Metals in the Environment: Toxic Metals Removal" *Bioinorganic Chemistry and Applications,* **2017.**
11. EPA Staff. "Drinking Water Requirements for States and Public Water Systems" **2017**. Web. https://www.epa.gov/dwreginfo/lead-and-copper-rule
12. Masten, Susan J., Simon H. Davies, and Shawn P. Mcelmurry. "Flint Water Crisis: What Happened and Why?"*J. Am. Water Works Assoc. ,***2016**. 108(12) 22–34.
13. Tchounwou P. B.; Yedjou C. G.; Patlolla A. K.; Sutton D. J.; "Heavy Metals Toxicity and the Environment" *EXS*. **2012**. 101:133-164.
14. Lenntech Staff, "Chemical properties of lead – Health effects of lead – Environmental effects of lead" **2018**. Web. https://www.lenntech.com/periodic/elements/pb.htm
15. McNeill, S; Goodyear, K.L.; "Bioaccumulation of heavy metals by aquatic macro-invertebrates of different feeding guilds: a review" *Science of The Total Movement.* 229(1) 1-19. **1999**
16. Mahurpawar, Manju. "Effects of Heavy Metals on Human Health" *Social Issues and Environment*. September, **2015**.
17. National Cancer Institute Staff. "Cancer Statistics" *NIH*. March 22, **2017**.
18. Assi, M. A., Hezmee, N. M. M., Haron, A. W., Sabri, Y. M. M., Rajion, M. A. "The detrimental effects of lead on human and animal health" *Vet. World.* **2016** 9(6): 660-671
19. Lidsky T.I, Schneider J.S. "Lead neurotoxicity in children:Basic mechanisms and clinical correlates" *Brain*. **2003**. 126(1):5–19

20. Garza A, Vega R, Soto E. "Cellular mechanisms of lead neurotoxicity" *Med. Sci. Monit.* **2006**. 12(3):57–65.
21. Agency for Toxic Substances & Disease Research "Lead Toxicity: What Are Possible Health Effects from Lead Exposure?" **2017**. Web. https://www.atsdr.cdc.gov/csem
22. Bisht, R., Agarwal, M., Singh, K. "Methodologies for removal of heavy metal ions from wastewater: an overview" *Interdiscinplinary Envir. Rev.* **2017**. 18: 124-142
23. "Filtration explained: How Do Brita Filters Work?" **2019**. Web. https://www.brita.com/why-brita/health/how-do-brita-filters-work
24. Barakat, M. A. "New trends in removing heavy metals from industrial wastewater" *Arabian Journal of Chemistry*. **2011**. 4(4): 361-377.
25. Lillerud, K. P., Cavka, J. H., Jakobsen, S., Olsbye, U., Guillou, N., Lamberti, C., Bordiga, S. "A New Zirconium Inorganic Building Brick Forming Metal Organic Frameworks with Exceptional Stability" *J. Am. Chem. Soc.* **2008**. 130, 13850-13851
26. Yaghi, O. M.; Furukawa, H.; Cordova, K.E.; O'Keefe, M.; "The Chemistry and Applications of Metal-Organic Frameworks" *Science*. **2013.** 341(6149):1230444-12
27. Li, J-R.; Kuppler, R. J.; Zhou, H-C.; "Selective gas adsorption and separation in metal-organic frameworks" *Chem. Soc. Rev*., **2009**,38, 1477-1504
28. Canivet, J.; Fateeva, A.; Guo, Y.; Coasne, B.; Farrusseng, D.; "Water adsorption in MOFs: fundamentals and applications" *Chem. Soc. Rev.,* **2014**, 43, 5594
29. Samanta, P.; Desai, A. V.; Sharma, S.; Chandra, P.; Ghosh, S. K. "Selective Recognition of Hg^{2+} ion in Water by a Functionalized Metal-Organic Framework (MOF) Based Chemodosimeter". *Inorg. Chem.* **2018**, 57, 2360-2364.
30. Luo, X.; Ding, L.; Luo, J. "Adsorptive Removal of Pb(II) Ions from Aqueous Samples with Amino-Functionalization of Metal-Organic Frameworks MIL-101(Cr)". *J. Chem. Eng. Data*. **2015**, 60, 1732-1743.
31. Pardo, E.; Mon, Marta, Lloret, F.; Ferrando-Soria, J.; Marti-Gastaldo, C.; Armentano, D. "Selective and Efficient Removal of Mercury from Aqueous Media with the Highly Flexible Arms of a BioMOF". *Angew. Chem. Int. Ed.*. **2016**, 55, 11167-11172.
32. Samanta, P.; Desai, A. V.; Sharma, S.; Chandra, P.; Ghosh, S. K. "Selective Recognition of Hg^{2+} ion in Water by a Functionalized Metal-Organic Framework (MOF) Based Chemodosimeter." *Inorg. Chem.*, **2018**, 57, 2360-2364
33. Chakraborty, A.; Bhattacharyya, S.; Hazra, A.; Ghosh, A. C.; Maji, T. K.; "Post-synthetic metalation in an anionic MOF for efficient catalytic activity and removal of heavy metal ions from aqueous solution" *Chem. Commun*., **2016**,52, 2831-2834
34. Liu, X.; Demir, N. K.; Wu, Z.; Li, K.; "Highly Water-Stable Zirconium Metal–Organic Framework UiO-66 Membranes Supported on Alumina Hollow Fibers for Desalination" *J. Am. Chem. Soc.* **2015**, 137(22), 6999-7002
35. Farha, O. K. *et al.* "Water-Stable Zirconium-Based Metal-Organic Framework Material with High-Surface Area and Gas-Storage Capacities" **2014**, 20(39) 12389-12393
36. Li, K.; Wang, C.; Liu, X.; Demir, N. K.; Chen, P.; "Applications of Water Stable Metal-Organic Frameworks" *Chem. Soc. Rev*., **2016**, 45, 5107-5134
37. Mikirova, N.; Casciari, J.; Hunninghake, R. "Efficacy of oral DMSA and intravenous EDTA in chelation of toxic metals and improvement of the number of stem/progenitor cells in circulation" *Translational Biomedicine*. **2011** Vol. 2
38. Harris, S.; "Understanding the binding and activation of thiophenic molecules in transition metal complexes and clusters" *Polyhedron,* 16(20): 3219-3233

39. Bu, X.; Zhang, J.; Chen, S.; Wu, T.; Feng, P.; "Homochiral Crystallization of Microporous Framework Materials from Achiral Precursors by Chiral Catalysis" *J. Am. Chem. Soc.* **2008**. 130(39): 12882-12883
40. Yaghi, O. M.; Eddaoudt, M.; Kim, J.; Vodak, D.; Sudik, A.; Wachter, J.; O'Keeffe, M.; "Geometric requirements and examples of important structures in the assembly of square building blocks" *PNAS*. **2002**, 99(8): 4900-4904
41. Low, J. J.; Benin, A. I.; Jakubczak, P.; Abrahamian, J. F.; Faheem, S. A.; Willis, R. R. "Zeolite-like Metal−Organic Frameworks (ZMOFs) as Hydrogen Storage Platform: Lithium and Magnesium Ion-Exchange and H_2-(rho-ZMOF) Interaction Studies" *J. Am. Chem. Soc*., **2009**, 131: 2864-2870
42. Kaskel, S.; Bon, V.; Senkovska, I.; Baburin, I. A.; "Zr- and Hf-Based Metal-Organic Frameworks: Tracking Down the Polymorphism*" Cryst. Growth. Des*. **2013**, 13(3): 1231-1237
43. Wu, H.: Chua, S.; Krungleviciute, V.; Tyagi, M.; Chen, P.; Yildirim, T.; Zhou, W.; "Unusual and Highly Tunable Missing-Linker Defects in Zirconium Metal-Organic Framework UiO-66 and Their Important Effects on Gas Adsorption" *J. Am. Chem. Soc.* **2013**, 135(28): 10525-10532
44. Jutzi, P.; Burford, N.; "Structurally Diverse π-Cyclopentadienyl Complexes of the Main Group Elements" *Chem. Rev.*, **1999**, 99: 969-990
45. Exner, M. M.; Waack, R.; Steiner, E. C. "Studies of Solvent Effects on the Nature of Ion Pair Interaction in 9-(2-Hexyl)fluorenyllithium" *J. Am. Chem. Soc.* **1973**, 95: 7009-7018.
46. Schleyer, P. v. R.; Jiao, H. "What is aromaticity?" *Pure Appl. Chem*. **1996**: 68, 209-218.
47. Paquette, L. A.; Bauer, W.; Sivik, M. R.; Buhl, M.; Feigel, M.; Schleyer, P. v. R. "Structure of lithium isodicyclopentadienide and lithium cyclopentadienide in tetrahydrofuran solution. A combined NMR, IGLO, and MNDO study" *J. Am. Chem. Soc.* **1990**, 112: 8776-8788.
48. Haigh, C. W.; Mallion, R. B. "Ring Current Theories in Nuclear Magnetic Resonance" *Prog. Nucl. Mag. Res. Sp.,* **1980**, 13: 303-344
49. Woldeamanuale, T.B. "Iron, colbalt, and nickel-ligand bonding in metallocene: Differentiation between bonds stability and reactivity" *IJCMP*. **2017**, 1-19